Tectonophysics 476 (2009) 371–396

Contents lists available at ScienceDirect

Tectonophysics

journal homepage: www.elsevier.com/locate/tecto

Review article

A systematic compilation of earthquake precursors

Robert D. Cicerone [a,*], John E. Ebel [b], James Britton [b,c]

[a] Department of Earth Sciences, Bridgewater State College, Bridgewater, MA 02325, USA
[b] Weston Observatory, Department of Geology and Geophysics, Boston College, 381 Concord Road, Weston, MA 02493-1340, USA
[c] Weston Geophysical Corporation, 181 Bedford Street, Suite 1, Lexington, MA 02420, USA

ARTICLE INFO

Article history:
Received 9 September 2008
Received in revised form 20 May 2009
Accepted 4 June 2009
Available online 13 June 2009

Keywords:
Earthquake prediction
Earthquake precursors
EM fields
Gas emissions
Surface temperatures
Surface deformations
Seismicity
Seismic hazard

ABSTRACT

A survey of published scientific literature was undertaken to identify and catalog observed earthquake precursors. The earthquake precursors selected for analysis included electric and magnetic fields, gas emissions, groundwater level changes, temperature changes, surface deformations, and seismicity. For each of these precursors, the published scientific literature was searched to document the statistics of each reported earthquake precursor (spatial extent, time, duration, amplitude, signal/noise ratio), to analyze dependence of the observable for each precursor on earthquake magnitude, and to explore proposed physical models to explain each earthquake precursor. Some general characteristics were observed for these precursory phenomena. First, the largest amplitude precursory anomalies tend to occur before the largest magnitude earthquakes. Also, the number of precursory anomalies tends to increase the closer in time to the occurrence of the earthquake. Finally, the precursory anomalies tend to occur close to the eventual epicenter of the earthquake. In general, the physical models indicate that all of the precursory phenomena are related to deformation that occurs near the fault prior to the main earthquake. While the models provide plausible physical explanations for the precursors, there are many free parameters in the models that are poorly resolved.

Contents

* Corresponding author. Tel.: +1 508 531 2713; fax: +1 508 531 1785.
E-mail address: rcicerone@bridgew.edu (R.D. Cicerone).

0040-1951/$ – see front matter © 2009 Elsevier B.V. All rights reserved.
doi:10.1016/j.tecto.2009.06.008

1. Introduction

One of the more elusive goals in seismology is short-term earthquake prediction. By the mid 1970s, seismologists were confident that short-term earthquake prediction would be achieved within a short period of time. This confidence came about in part as the result of the first successful prediction of a large earthquake, the 1975 M7.4 Haicheng earthquake in China. Because of this prediction, an alert was issued within the 24-hour period prior to the main shock, probably preventing a larger number of casualties than the 1328 deaths that actually occurred from this event. However, the failure to predict another devastating earthquake 18 months later, the 1976 M7.8 Tangshan earthquake, was a major setback to the earthquake prediction effort. Casualties from this earthquake numbered in the hundreds of thousands. A summary of these events, as well as other successes and failures in earthquake prediction, is given by Lomnitz (1994).

One area that may hold promise in advancing the science of short-term earthquake prediction is the study of earthquake precursors. In fact, short-term predictions are typically based on observations of these types of phenomena. The term *earthquake precursor* is used to describe a wide variety of physical phenomena that reportedly precede at least some earthquakes. These phenomena include induced electric and magnetic fields, groundwater level changes, gas emissions, temperature changes, surface deformations, and anomalous seismicity patterns. While each of these phenomena has been observed prior to certain earthquakes, such observations have been serendipitous in nature. For example, anomalous magnetic fields were recorded prior to the 1989 Loma Prieta earthquake in California by a magnetometer installed to monitor electromagnetic noise produced by electric trains. Fortuitously, this magnetometer was located within 7 km of the epicenter of the Loma Prieta earthquake (Fraser-Smith et al., 1990). The magnetometer detected two precursory magnetic fields, the first approximately 2 weeks prior to the main shock and the second approximately 3 h before the main shock.

More recently, attempts have been made to monitor various precursory phenomena as part of an overall earthquake prediction effort. The Parkfield, CA experiment (Bakun and Lindh, 1985) is one such experiment. A wide array of geophysical instruments was installed along a segment of the San Andreas Fault in central California (the so-called Parkfield segment) in 1981. These instruments included magnetometers, water level monitors, creepmeters, and straimeters and were designed to record a wide variety of precursory phenomena. Based on magnitude 6+ earthquakes on the San Andreas Fault at Parkfield from 1857 to 1966, the United States Geological Survey (USGS) issued an official prediction of a M6 earthquake along this segment in 1985, to occur with 95% probability before the end of 1993 (Working Group on California Earthquake Probabilities, 1988). This earthquake did not occur until late 2004, and no precursory phenomena of significance were observed. A preliminary report on this earthquake and its lack of precursors is given by Langbein et al. (2005).

The purpose of this study was to carry out a survey of published scientific literature to identify and catalog observed earthquake precursors that have been published. In this work we identified several types of earthquake precursors and searched the published scientific literature to carry out the following tasks:

- Document the statistics of each reported earthquake precursor (spatial extent, time, duration, amplitude, signal/noise ratio)
- Analyze the dependence of the observable for each precursor on earthquake magnitude
- Explore proposed physical models to explain each earthquake precursor

This report summarizes the results of this research and presents recommendation for follow-up research. With an eye toward future earthquake prediction research, the potential of observing the reported earthquake precursors from a space-based remote-sensing platform is assessed.

2. Selection of earthquake precursors

Two major criteria were used to select the earthquake precursors for this study. The first criterion used for the selection of the earthquake precursory observables was the reported existence of credible scientific evidence for anomalies in the observables prior to at least some earthquakes. As noted above, the successful measurement of some anomalous phenomenon prior to an earthquake usually depends on the luck of having a good scientific experiment operating in an area before, during and after an earthquake. In many cases there have been anecdotal reports of unusual phenomena before earthquakes (e.g., unusual groundwater level changes or unusual animal behavior), but these have not been documented scientifically in a quantitative way. In order to best summarize the behavior of precursory phenomena of interest, we sought out those studies from the published scientific literature that report observations of earthquake precursors that were observed in credible, controlled, calibrated experiments.

The second criterion for the selection of the earthquake precursors is that there are accepted physical models to explain the existence of the precursor. For example, it only makes sense to look for changes in the local electric or magnetic field near an earthquake epicenter if there is some physical or chemical reason why the time prior to the initiation of an earthquake rupture should be accompanied by those field changes. In some cases, there are multiple, competing models to explain the existence of a reported earthquake precursor. We used these competing models as evidence that there is some physical model to explain the precursor, even if there is no current scientific agreement about which model is best.

The earthquake precursors selected for analysis in this study were

- *Electric and magnetic fields* — localized changes in magnetic and electric fields (including changes in ULF, VLF, ELF and RF fields). There is the uncontested observation of a localized strong ULF field change that took place in the area of the 1989 Loma Prieta, California earthquake (magnitude 7.1) during the hours prior to the main shock. A weaker field change was observed about 2 weeks before the main shock.
- *Gas emissions* — there is a great deal of interest in the emissions of various gases from the earth prior to earthquakes. The most well-known experiments have focused on radon gas, but some experiments have measured changes in the emission of other gases from the earth.
- *Water level changes* — wells have been reported to change levels or water quality in the hours, days or weeks prior to a number of earthquakes. In fact, well-water level changes is one of the most commonly reported earthquake precursors.
- *Temperature changes* — there have been some reports of surface temperature changes prior to earthquakes. These may involve changes in the circulation patterns of groundwater bringing water of different temperature to the surface.
- *Surface deformations* — there have been reports that changes in ground elevations over distances of tens of kilometers have preceded

some strong earthquakes. The number of permanent, high quality GPS sites to monitor permanent ground deformations is increasing in earthquake-prone areas, but broadscale remote sensing of surface elevations and especially elevation changes could yield important new clues for predicting earthquakes.

- *Seismicity* — this is already well covered by surface-based seismic instrumentation. However, some high-frequency (acoustic emission) energy and very low frequency seismic motions not detected by conventional seismographs may provide important precursory information. For example, Ihmle and Jordan (1994) have shown that some earthquakes exhibit low frequency precursory signals prior to the higher frequency main rupture.

3. Method of data analysis

For each of the earthquake precursors defined in the previous section, two different research tasks were conducted. The first was to carry out a survey of the scientific literature to find studies documenting anomalous changes in one or more of the selected precursors prior to the occurrence of an earthquake. From these studies, several types of information about the anomalous precursory signal were sought. These included the length of time before the earthquake when the precursor initiated, the duration of the precursor, the amplitude of the precursory signal, the signal-to-noise ratio of the anomalous relative to normal background noise, and the distance from the observation point to the earthquake. In addition, some basic source information was collected for each earthquake, including the date, time, location and magnitude of the earthquake. For each type of precursor, the observational information from the literature survey was collected and analyzed to find the statistical properties of the initiation and duration of the precursors, the strength of the precursory signal, and the relation of the precursory signal properties to the magnitude of the earthquake and the distance from the observation point to the source.

The second research task was to survey the scientific literature for studies proposing physical models to explain each of the precursors. Each physical model was evaluated to see if it predicted pre-earthquake anomalies consistent with the observations collected in the first research task. The goal of this aspect of the research was to find realistic physical models of the precursory earthquake signals that can be used to estimate the strength and character of anomalous pre-earthquake signals for each of the earthquake precursors. In particular, this aspect of the analysis is necessary to determine the importance of such earthquake source properties as magnitude, seismic moment, focal mechanism, depth, and stress drop in generating precursory signals.

4. Summary of the earthquake precursors: observations and models

This section presents a summary of the data collected for each of the precursors analyzed in this study. The reported observations for each precursor for each earthquake are summarized in tables. Discussions of the observations are given in each subsection here. Also described in each subsection are the results of the search for the physical models to explain the earthquake precursor observations. Those models are explored to determine their consistency with the reported precursor observations.

4.1. Electric and magnetic field observations

Anomalous electric and magnetic field prior to earthquakes have been detected by both ground-based and satellite-based instruments. In fact, this is the one earthquake precursor for which satellite-based observations have been reported in the literature. Those satellite observations come from two different studies. The first is a Russian study of an earthquake on March 19, 1979, where Larkina et al. (1989) reported that the Intercosmos 19 satellite detected changes in the ionospheric ELF and VLF emissions at 800 Hz and 4650 Hz from 8 h before to 3 h after each earthquake in their data set. The anomalously large amplitudes at these two frequencies were detected within 2° latitude and 60°longitude of the eventual epicenter of the earthquake.

The second satellite-based EM study of precursory earthquake emissions was reported by Serebryakova et al. (1992). In that study ELF/VLF signals from the COSMOS-1809 satellite were analyzed to look for signals associated with aftershocks of the 1988 earthquake in Armenia. Serebryakova et al. (1992) found that EM radiation at frequencies below 450 Hz was observed during 12 of the 13 orbital passes of the satellite within 6° of longitude of the aftershock epicenter. The anomalously strong emissions were not observed at the latitude of the epicenters of earthquakes but rather 4° to 10° south of those epicenters. The emissions were observed up to a few hours before strong aftershocks took place in the epicentral region. Serebryakova et al. (1992) report that similar anomalous radiation was detected in this same area by the AUREOL-3 satellite.

Finally, Parrot (1994) described a statistical study of ELF/VLF emissions recorded by the AUREOL-3 satellite in the vicinity of the epicenters of 325 earthquakes of Ms > 5 from 1981–1983. In order to maximize the strength of the signals analyzed, Parrot (1994) averaged the data over time, thus sacrificing the time resolution in his study. He reported that the EM signal strength is at a maximum within 10° of longitude of the earthquake epicenters and that these signals are observed at all latitudes. The temporal averaging of the data precluded determining whether the anomalous signals occurred prior to, coincident with, or subsequent to the earthquakes that were analyzed.

There are some important ground-based observations that support the idea that the earth can generate anomalous electric and magnetic signals prior to the occurrences of earthquakes. The most important is that of Fraser-Smith et al. (1990) who, quite by accident, detected a strong ULF magnetic field change near the epicenter of the 17 October 1989 Ms 7.1 Loma Prieta, California earthquake. A low frequency (0.5–2.0 Hz), low amplitude increase in the background ULF field strength began being recorded about a month before the earthquake by an instrument placed at Corralitos (7 km from the eventual epicenter) to monitor ULF background noise for purposes not related to seismology. About 2 weeks before the earthquake, the background ULF signal detected by the instrument increased noticeably. Finally, within a few hours of the earthquake there was an exceptionally great increase in the signal amplitude at frequencies of 0.01 to 0.5 Hz, which grew continuously until the occurrence of the earthquake (and power was lost to the instrument). Atmospheric disturbances as the cause of the anomalous signals were ruled out, and it appears likely that the signals observed were generated by magnetic field changes in the earth below the instrument. Curiously, an ELF/VLF instrument operating about 52 km away on the Stanford U. campus detected no anomalous signals during this same time period.

Also supporting the idea that earthquakes are associated with magnetic and electric field changes in the rock is a study by Kopytenko et al. (1993) who reported unusual ULF signals at a ground-based observatory within 200 km of the epicenter of the 1988 Armenia earthquake. They reported that anomalous ULF emissions were detected several hours before the Armenia main shock and some of its strong aftershocks. This is the same aftershock sequence analyzed by Serebryakova et al. (1992).

As is clear from the discussion here and the results summarized in Table 1, there are still many uncertainties in the observations of possible precursory EM emissions associated with strong earthquakes. Some satellite frequency bands seem to see anomalous signals, while others do not. One study reports the signals at a wide range of latitudes and a narrow range of longitudes, while another sees the opposite pattern. However, all of the data, including the best ground-based observations, show that precursory signals can be observed within several hours of a coming earthquake and that those signals seem to be strongest near the coming epicenter. The Loma Prieta observations suggest that signal-to-noise ratios of anomalous ULF

Table 1
Reported precursory electric and magnetic fields associated with earthquakes.

Earthquake	Magnitude	Date	Type of emission	Before (b)/during (d)/after (a)?	Frequency range	Signal level	Background level	SNR	Distance from epicenter (km)	Instrumentation	Reference
Chile	9.5	5/22/1960	Radio	b (6 days)	18 MHz	2.56×10^{-6} W/Hz			Worldwide	radio astronomy receiver	Warwick et al., 1982
Worldwide (13 events)	5.7–8.3	1964–1973	Geomagnetic	b (<1 h)							Gogatishvili,1984
San Andreas Fault, California	3.9	6/22/1973	Electrical resistivity variation	b (2 months)	DC	10% increase			4 km	Dipole–dipole array	Mazzella and Morrison, 1974
Hollister, California	5.2	11/28/1974	ULF magnetic	b (7 weeks–several months)		0.9–1.5 nT			11 km	Array of 7 proton-precession magnetometers	Smith and Johnston, 1976
Haicheng, China	7.3	2/4/1976	Electric	b (12 h)		−150 mV			20 km		Savage, 1977
Tangshan, China	7.8	7/28/1976	Resistivity	b (2–3 years)		3–5% decrease			≤ 150 km		Zhao and Qian, 1994
Tangshan, China	7.8	7/28/1976	Self potential	b (3 months)		3 mV/km increase			≤ 120 km		Zhao and Qian, 1994
Sungpan–Pingwu, China (3 events)	7.2 6.8 7.2	8/16/1976 8/22/1976 8/23/1976	Telluric currents	b (1 month)		20–50 μA			≤ 200 km		Wallace and Teng, 1980
Worldwide (8 events)	5.0–6.1	1979–1980	VLF EM	b (26–183 min)	0.1–16 kHz				700–14,100 km	Interkosmos–19 satellite	Larkina et al., 1984
Kyoto, Japan	7.0	3/31/1980	VLF electric	b (1/2 h)	81 kHz	+15 dB			250 km	Electric antenna	Gokhberg et al., 1982
Tokyo, Japan	5.3	9/25/1980	VLF electric	b (1 h)	81 kHz	+15–20 dB			55 km	Electric antenna	Gokhberg et al., 1982
Tokyo, Japan	5.0	1/28/1981	VLF electric	b (3/4 h)	81 kHz	+12 dB			50 km	Electric antenna	Gokhberg et al., 1982
Greece (47 events)	3.4–6.8	1983	Electric	b		0.2–15.6 mV			10–160 km		Varotsos and Alexopoulos, 1984
Japan (26 events)	5.0–6.6	1985–1990	VLF electric	b (up to 2 days)	82 kHz				2–895 km	Loop antennas	Yoshino et al., 1993
Kalamata, Greece	6.2	9/13/1986	Electric	b (3–5 days)		10s mV			200 km		Gershenzon and Gokhberg, 1993
Spitak, Armenia	6.9 Ms	12/7/1988	ULF magnetic	b (4 h), a	0.01–1 Hz	0.2 nT	0.02 nT	10	128 km	3-axis high-sensitivity magnetometers	Molchanov et al., 1992
Spitak, Armenia	6.9 Ms	12/7/1988	ULF magnetic	b (4 h), a	0.005–1 Hz	0.1–0.2 nT	0.03 nT	6.67	120 km and 200 km		Kopytenko et al., 1993
Ito, Japan (earthquake swarm)	≤5.5	June–July 1989	ELF/VLF electric	b (4–6 h)	1–9 kHz	~10 mV			200 km	Borehole electrodes	Fujinawa and Takahashi, 1990
Loma Prieta, California	7.1 Ms	11/19/1989	ELF/VLF EM	b (3 h), d	0.01 Hz	5–60 nT $Hz^{-1/2}$	~1 nT $Hz^{-1/2}$		52 km	Ground-based magnetometers	Fraser-Smith et al., 1990
Loma Prieta, California	7.1 Ms	11/18/1989	ULF magnetic	b (3 h), a	0.01 Hz	4–5 nT			7 km		Molchanov et al., 1992
Loma Prieta, California	7.1 Ms	11/18/1989	ULF magnetic	a	0.01–10 Hz	1 nT			7.3 km	Proton magnetometers	Mueller and Johnston, 1990
Armenia region		1989	ELF/VLF EM	b (3 h)	140 Hz	10 mγ			6 in. long, 2–4 in latitude	COSMOS-1809 satellite	Serebryakova et al., 1992
Armenia region		1990	ELF/VLF EM	b (3 h)	450 Hz	3 mγ			6 in long, 2–4 in latitude	COSMOS-1809 satellite	Serebryakova et al., 1992
Worldwide (325 eq's)	Ms>5		ELF/VLF EM	b (0–4 h)	140 Hz	3.28E−5 γ $Hz^{-1/2}$	1.53E−5 γ $Hz^{-1/2}$	2.14	Δlong<10	ARCAD-3 aboard AUREOL-3 satellite	Parrot, 1994
Worldwide (325 eq's)	Ms>5		ELF/VLF EM	b (0–4 h)	800 Hz	9.08E−5 γ $Hz^{-1/2}$	1.57E−5 γ $Hz^{-1/2}$	5.78	Δlong<10	ARCAD-3 aboard AUREOL-3 satellite	Parrot, 1994
Worldwide (325 eq's)	M>5.5		LF radio wave			10^2–10^3 V m^{-1}			60 in long, 2 in latitude	Intercosmos-19 satellite	Parrot, 1994
Upland, California	4.7	4/17/1990	ELF magnetic	b (1 day)	3.0–4.0 Hz	−40 dB	−46.8 dB		160 km	Vertical magnetic sensor	Dea et al., 1993
Western Iran	7.5	6/20/1990	Ionospheric (radio wave)	b (16 days)	0–8 kHz, 10–14 kHz, F region				250–2000 km	Intercosmos-24 satellite	Shalimov and Gokhberg, 1998

Watsonville, California	4.3	3/23/1991	ELF magnetic	b (data averaged over 2 days)	3.0–4.0 Hz	−43 dB	−47.6 dB		600 km	North–south magnetic sensor	Dea et al., 1993
Watsonville, California	4.3	3/23/1991	ELF magnetic	b (data averaged over 2 days)	3.0–4.0 Hz	−44 dB	−46.8 dB		600 km	Vertical magnetic sensor	Dea et al., 1993
Coalinga, California	4.0	1/15/1992	ELF magnetic	b (data averaged over 2 days)	3.0–4.0 Hz	−50 dB	−57 dB		400 km	Vertical magnetic sensor	Dea et al., 1993
Central Italy	3.0–4.3	1991–1994	LF radio waves	b (6–10 days)	216 kHz	−21 to −22 db (atmospheric) −7 to −5 db (ground)			<100 km		Bella et al., 1998
Hokkaido, Japan	7.8	7/12/1993	foF_2 ionospheric	b (3 days)					290 km, 780 km, 1280 km (3 stations)		Ondoh, 1998
Guam	Ms 7.1	8/8/1993	ULF magnetic	b (1 month)	0.02–0.05 Hz	0.1 nT			65 km	3-axis ring–core-type fluxgate magnetometer	Hayakawa et al., 1996; Hayakawa et al., 1999
Mexico (Pacific Coast)	$M \geq 6.0$ (4 events)	1993–1994	ULF electric		0–0.125 Hz				< 200 km		Yépez et al., 1995
Hokkaido–Toho–Oki, Japan	M_W 8.1	10/4/1994	VLF electric	b (20 min)	1–9 kHz	1.34 mV			> 1000 km	Borehole antenna	Fujinawa and Takahashi, 1998
Taiwan	$M \geq 6.0$ (14 events)	1994–1999	ULF magnetic	b (1–6 days)					<400 km	IPS-42 ionosonde	Liu et al., 2000
Hyogo-ken Nanbu (Kobe), Japan	7.2	1/17/1995	DC geopotential, ELF magnetic, VLF radio, MF–HF, VHF FM-wave	b (up to 7 days)	223 z, 1–20 kHz, 163 kHz, 77.1 MHz				≥ 100 km		Enomoto et al., 1998
Hyogo-ken Nanbu (Kobe), Japan	7.2	1/17/1995	VLF radio	b (2 days)	10.2 kHz				70 km		Molchanov et al., 1998
Hyogo-ken Nanbu (Kobe), Japan	7.2	1/17/1995	Electric	b (1 h)	22.2 MHz	0.2 W signal power			77 km	Phase-switched interferometer with two horizontally-polarized antennas	Maeda and Tokimasa, 1996
Kozani-Grevena, Greece	6.6	5/13/1995	VHF electromagnetic	b (20 h)	*E*: 41 and 5 MHz *M*: 3 & and 10 kHz	~300 mV above background			Δlat, Δlong <3	Electric dipole antennas, magnetic loop antennas	Eftaxias et al., 2002
Kozani-Grevena, Greece	6.6	5/13/1995	Electric, magnetic	b (2 weeks)		10–60 mV/km, 0.4 nT			70 m, 200 km		Bernard et al., 1997
Biak, Indonesia	8.2	2/17/1996	UHF magnetic	b (1–1.5 months)	5–30 mHz	0.2–0.3 nT			≤ 1200 km	Fluxgate magnetometers	
Chiba-ken Toko-oki, Japan	6.2	9/11/1996	VHF electric	b (3 days)					320, 430 km	Vertical-dipole ground electrodes	Enomoto et al., 1997
Akita-ken Nairiku-Nanbu, Japan	5.9	8/11/1996	VHF electric	b (6 days)					<100 km	Vertical-dipole ground electrodes	Enomoto et al., 1997
Vrancea, Romania	*M* (3.9 (19 events)	1997–1998	ULF electromagnetic	b (1–12 days)	3 kHz		~15 pT $Hz^{-1/2}$		100 km	3-axis fluxgate magnetometers, non-polarizable electric sensors	Enescu et al., 1999
Umbria–Marche, Italy	5.5	3/26/1998	LF radio	b (1.5 months)	0.006 Hz	6–8 dB increase			818 km	Radio wave vertical antenna	Biagi et al., 2001
San Juan Bautista, California	MW 5.1	8/12/1998	UHF magnetic	b (2 h)	0.01–10 Hz	0.02 nT			3 km	3-component magnetic field inductor coils	Karakelian et al., 2002
Athens, Greece	5.9	9/7/1999	VHF electromagnetic	b (12–17 h)	*E*: 41 and 5 MHz *M*: 3 and 10 kHz	(300 mV above background)		6	Δlat, Δlong <3	Electric dipole antennas, magnetic loop antennas	Eftaxias et al., 2001a,b
Chi-Chi, Taiwan	7.7	9/20/1999	ULF magnetic	b (1, 3, 4 days) 3 signals					< 400 km	IPS-42 ionosonde	Liu et al., 2000
Chi-Chi, Taiwan	M_W 7.6	9/20/1999	foF_2 ionospheric	b (3–4 days)					120 km	IPS-42 ionosonde	Chuo et al., 2002
Chia-Yii, Taiwan	M_W 6.4	10/22/1999	foF_2 ionospheric	b (1–3 days)					179 km	IPS-42 ionosonde	Chuo et al., 2002
Japan	*M* (4.8 (29 events)	9/4/2001–4/8/2003	VHF electromagnetic	b (up to 5 days)					Δlat Δlong <4	Two 5-element Yagi antennas	Fujiwara et al., 2004

fields associated with coming earthquakes can be quite strong (up to 60). The three satellite-based studies described above report signal-to-noise ratios up to 10. Thus, EM radiation significantly above the background noise prior to at least some earthquakes may be observable from space in carefully designed experiments.

4.2. Electric and magnetic field models

Several physical models have been proposed to explain the observed electromagnetic precursors associated with earthquakes. These models can be classified into two main categories, which can be related to the frequency of the resultant electromagnetic precursor. The first class of models attempts to explain the observation of magnetic fields in the ULF range. The second class of models relates to electric fields observed at higher frequency, principally in the ELF/VLF range, but also extending to the LF and HF frequency bands.

4.3. ULF magnetic fields

For ULF magnetic fields, there have been three mechanisms proposed to explain the generation of these precursory signals. The first of these mechanisms is the magnetohydrodynamic (MHD) effect (e.g., Draganov et al., 1991). For this mechanism, the flow of an electrically conducting fluid in the presence of a magnetic field generates a secondary induced field. The MHD equation is derived from Maxwell's equations and is given by

$$\frac{\partial \mathbf{B}}{\partial t} = \nabla \times \mathbf{v} \times \mathbf{B} + \frac{\nabla^2 \mathbf{B}}{\mu_0 \sigma}, \tag{1}$$

where μ_0 is the permeability of free space, s is the conductivity, $\mathbf{v}$ is the fluid velocity, and $\mathbf{B}$ is the magnetic field. The first term on the right is the convection of the magnetic field caused by the resistance to flux changes in the conductive loop. The second term represents the diffusion of the magnetic field caused by ohmic dissipation.

From the two terms on the right-hand side of the MHD equation, a magnetic Reynolds number R_m, analogous to the hydrodynamic Reynolds number, can be defined. The Reynolds number defines the relative importance of the convective and diffusive terms. Using dimensional analysis,

$$R_m = \frac{|\nabla \times \mathbf{v} \times \mathbf{B}|}{|\lambda \nabla^2 \mathbf{B}|} = \mu_0 \sigma v \ell, \tag{2}$$

where $\lambda = 1/\mu_0\sigma$ and ℓ is the characteristic length of the source. Then the induced magnetic field $\mathbf{B}_i$ is given by

$$\mathbf{B}_i = R_m \mathbf{B}. \tag{3}$$

The second mechanism proposed for the generation of precursory ULF magnetic fields is the piezomagnetic effect (e.g., Sasai, 1991). For this mechanism, a secondary magnetic field is induced due to a change in magnetization in ferromagnetic rocks in response to an applied stress. For an isotropic material, the change in magnetization ΔM_i due to the piezomagnetic effect is given by

$$\Delta M_i = \left(-\frac{1}{2}\tau_{kk}\delta_{ij} + \frac{3}{2}\tau_{ij}\right)\beta M_j, \tag{4}$$

where β is the stress sensitivity, τ is the stress tensor, and δ_{ij} is the Kronecker delta. If the material is linear elastic and obeys Hooke's law, the constitutive relation can be written as

$$\tau_{ij} = \lambda \delta_{ij} \nabla \cdot \mathbf{u} + \mu\left(\frac{\partial u_i}{\partial x_j} + \frac{\partial u_j}{\partial x_i}\right), \tag{5}$$

where λ and μ are the Lamé constants and $\mathbf{u}$ is the displacement vector. Substituting this constitutive law into the into the equation for the change in magnetization leads to a difference equation that can be numerically integrated to determine the magnetic field at the surface resulting from piezomagnetic effects.

The third mechanism proposed to explain the generation of ULF magnetic fields is the electrokinetic effect (Nourbehecht, 1963; Fitterman, 1978, 1979). The electrokinetic effect results from the flow of electric currents in the earth in the presence of an electrified interface at solid–liquid boundaries. These electric currents in turn produce magnetic fields. The current density and fluid velocity are coupled processes defined by

$$\mathbf{j} = -\sigma \nabla E - \frac{\varepsilon \varsigma}{\eta} \nabla P, \tag{6}$$

and

$$\mathbf{v} = -\frac{\varepsilon \varsigma}{\eta} \nabla E - \frac{k}{\eta} \nabla P, \tag{7}$$

where $\mathbf{j}$ is the current density, $\mathbf{v}$ is the fluid velocity, E is the streaming potential, ε is the dielectric constant, ς is the zeta potential (a measure of the initial potential at the electrified interface), σ is the fluid conductivity, η is the dynamic viscosity, k is the permeability, and P is the fluid pressure. The magnetic field $\mathbf{B}$ is induced by the flow of electric current and is given by the Biot–Savart law

$$\mathbf{B} = \frac{\mu_0}{4\pi} \int_V \int \int \frac{\nabla' \times \mathbf{j}(\mathbf{r}')}{|\mathbf{r} - \mathbf{r}'|} dV, \tag{8}$$

where μ_0 is the permeability of free space.

Fenoglio et al. (1994a,b; 1995) analyzed the relative contribution of these three mechanisms applied to the ULF magnetic field signals observed prior to the 17 October 1989 Loma Prieta earthquake (Fraser-Smith et al., 1990). The analysis focused on two major increases in the magnetic field prior to the earthquake, the first having a magnitude of 2.0 nT occurring on 5 October 1989 and the second of magnitude 6.7 nT occurring just 3 h prior to the earthquake.

The results of these studies indicate that the MHD effect has a negligible contribution to the ULF magnetic signal, due to the rapid attenuation of the magnetic field strength, which decays as $1/r^3$. The piezomagnetic effect contributes an induced magnetic field of at most 10^{-2} nT, approximately two orders of magnitude less than the observed signals. The electrokinetic effect appears to be the most significant, contributing an induced magnetic field of about 5–10 nT, of about the same order as the observed fields prior to the earthquake.

In contrast, Draganov et al. (1991) attributed the observed precursory ULF magnetic fields as being the result of magnetohydrodynamic effects. However, as pointed out by Fenoglio et al. (1995), the Draganov analysis used certain model parameters that were unrealistic. These include a value for the permeability k of 10^{12} m^2, a value which is approximately two orders of magnitude higher than would be expected for the rocks in the earthquake source region, and a pressure field of 4×10^{10} Pa, well above the lithostatic pressure at that depth (about 10^8 Pa).

4.4. ELF/VLF/LF/HF electric fields

As mentioned above, there have been several reports in the literature of anomalous electric fields in the ELF/VLF frequency ranges and higher. The mechanisms proposed for the generation of these fields include contact electrification, separation electrification, and piezoelectrification (Ogawa et al., 1985) and atmospheric electricity generated by the emission of radon gas from the earth (Pierce, 1976).

Ogawa et al. (1985) examined the electric field generated from granite samples that were struck with a hammer or fractured by bending. They attributed the generation of the electric field to two possible mechanisms: contact (or separation) electrification or piezoelectrification. These mechanisms create a dipole moment due to separation

Table 2
Reported precursory gas emissions associated with earthquakes.

Area (notes)	Country	Date	z [km]	Gas		δa [%]	Background level [cpm]	Signal level [cpm]	M	D [km]	d [days]	δt [days]	References
Southern (a)	Iceland	7/3/1978		Rn	+	380	Not given	Not given	2.7	14	22	25	Hauksson and Goddard, 1981
Iceland	Iceland	8/28/1978		Rn	+	60	Not given	Not given	3.4	5	17	30	Hauksson and Goddard, 1981
Seismic	Iceland	8/28/1978		Rn	+	280	Not given	Not given	3.4	21	17	27	Hauksson and Goddard, 1981
Seismic	Iceland	11/19/1978		Rn	−	80	Not given	Not given	4.3	16	18	10	Hauksson and Goddard, 1981
Seismic	Iceland	6/29/1979		Rn	+	40	Not given	Not given	1.9	9	19	25	Hauksson and Goddard, 1981
Seismic	Iceland	9/5/1979		Rn	+	40	Not given	Not given	2.8	8	17	20	Hauksson and Goddard, 1981
Seismic	Iceland	9/5/1979		Rn	+	100	Not given	Not given	2.8	5	33	33	Hauksson and Goddard, 1981
Tjörnes Facture Zone	Iceland	12/15/1979		Rn	+	100	Not given	Not given	4.1	56	50	50	Hauksson and Goddard, 1981
Tjörnes Facture Zone	Iceland	9/16/2002		Cu	+		0.91 ± 0.37 ppb	6.28 ($2\sigma = 2.54$)	5.8	100		1 week	Claesson et al., 2004
Tjörnes Facture Zone	Iceland	9/16/2002		Zn	+		26 ± 23 ppb	381 ppb ($2\sigma = 134$)	5.8	100		2 weeks	Claesson et al., 2004
Tjörnes Facture Zone	Iceland	9/16/2002		Mn	+		1.25 ± 0.35 ppb	6.76 ppb ($2\sigma = 2.91$)	5.8	100		5 weeks	Claesson et al., 2004
Tjörnes Facture Zone	Iceland	9/16/2002		Cr	+		2.8 ± 2.2 ppb	34 ppb ($2\sigma = 16$)	5.8	100		10 weeks	Claesson et al., 2004
Tjörnes Facture Zone	Iceland	9/16/2002		Fe	+		2.8 ± 2.2 ppb	28 ($2\sigma = 14.8$)	5.8	100		10 weeks	Claesson et al., 2004
Tjörnes Facture Zone	Iceland	9/16/2002		Na/Ca	+				5.8	100			Claesson et al., 2004
Tjörnes Facture Zone	Iceland	9/16/2002		B, Ca, K, Li, Mo, Na, Rb, S, Si, Sr Cl, SO_4	+	12–19%			5.8	100			Claesson et al., 2004
Tjörnes Facture Zone	Iceland	9/16/2002		$\delta^{18}O$	−	1.0 ± 0.1%			5.8	100			Claesson et al., 2004
Tjörnes Facture Zone	Iceland	9/16/2002		δD	−	9 ± 1%			5.8	100			Claesson et al., 2004
San Andreas fault	USA	3/17/1976	9	Rn	+	120	Not given	Not given	4.3	25	60	25	King, 1978; King, 1980
San Andreas fault	USA	1/19/1977	6	Rn	+	500	Not given	Not given	4	47	90	25	King, 1978; King, 1980
San Andreas fault	USA	12/15/1977	11	Rn	+	400	Not given	Not given	4	45	15	30	King, 1980
San Andreas fault	USA	8/29/1978	6	Rn	+	200	Not given	Not given	4.2	75	240	90	King, 1980
South California	USA	9/24/1977	15	Rn	+	44	Not given	Not given	2.9	21	1	5	Shapiro et al., 1980
South California	USA	12/20/1977	6	Rn	+	40	Not given	Not given	2.8	12	10	24	Shapiro et al., 1980
Malibu	USA	1/1/1979	?	Rn		4 spikes	Not given	Not given	4.6	54	4 spikes		Shapiro et al., 1980
Coalinga fault (b)	USA	6/7/1909		H_2	+	800	Not given	Not given	5.2 to 6.7	40–120			Sato et al., 1986
Kettleman Hill	USA	4/8/1985		Rn	+	100	Not given	Not given	5.6	300	10	7	Teng and Sun, 1986
Raquette Lake	USA			Rn			Not given	Not given	3.9	14			Fleischer, 1981
Blue Mountain Lake	USA			Rn			Not given	Not given	1.5	1			Fleischer, 1981
Pearblossom	USA	11/22/1976		Rn	+	36	Not given	Not given	3.5	25	31		Hauksson, 1981
Jocasse	USA	2/23/1977		Rn	−	50	Not given	Not given	2.3	1	14		Hauksson, 1981
Pasadena	USA	9/24/1977		Rn	+	62	Not given	Not given	2.9	21	3	5	Shapiro et al., 1980
Pasadena	USA	12/20/1977		Rn	+	25	Not given	Not given	2.8	12	9		Shapiro et al., 1980
Malibu	USA	1/1/1979		Rn	+	72	Not given	Not given	4.7	54	42		Shapiro et al., 1980
Malibu	USA	1/1/1979		Rn	+	225	Not given	Not given	4.7	20	82		Hauksson, 1981
Big Bear	USA	6/28/1979		Rn	+	310	Not given	Not given	5	85	12		Hauksson, 1981
Big Bear	USA	6/28/1979		Rn	+	72	Not given	Not given	5	31	45		Hauksson, 1981
Imperial Valley	USA	10/15/1979		Rn	+	400	Not given	Not given	6.6	335	116		Hauksson, 1981
Imperial Valley	USA	10/15/1979		Rn	+	200	Not given	Not given	6.6	310	95		Hauksson, 1981
Imperial Valley	USA	10/15/1979		Rn	+	72	Not given	Not given	6.6	265	145		Hauksson, 1981
Imperial Valley	USA	10/15/1979		Rn	+	64	Not given	Not given	6.6	260	2		Hauksson, 1981
Imperial Valley	USA	10/15/1979		Rn			Not given	Not given	6.6	300			Fleischer, 1981
Caruthersville, Missouri	USA	6/??/1979		Rn	+	375	not given	Not given	3.9	nd	33	60	Steele, 1981
Caruthersville, Missouri	USA	8/??/1981		Rn	+	340–504			4.0	40	5 months	2–7 months	Steele, 1984
Central Arkansas (earthquake swarm)	USA	1/??/1982		Rn	−				4.0–4.5	160	1 year	1 year	Steele, 1984
SW Illinois	USA	5/15/1983		Rn	+	483			4.2	120–320	2 months		Steele, 1984
New Madrid Seismic Zone	USA	1/28/1983		Rn	+	400			3.5	50	2 months		Steele, 1984
Big Bear, California	USA	6/30/1979		Rn	+	60	Not given	Not given	4.8	30	150	120	Chung, 1985
	USA			He	+	65	Not given	Not given	4.8	30	150	120	Chung, 1985
Alandale, California	USA	6/??/1983		Rn	+	1200	not given	Not given	3.7	13	3	15	Shapiro et al., 1985

(continued on next page)

Table 2 (*continued*)

Area (notes)	Country	Date	z [km]	Gas		δa [%]	Background level [cpm]	Signal level [cpm]	M	D [km]	d [days]	δt [days]	References
San Andreas, California	USA	10/13/1979		Rn	+	400	Not given	Not given	3.4	40	0.5	0.2	King, 1985
	USA	12/22/1979		Rn	+	800	Not given	Not given	3.3	20	1	0.5	King, 1985
Loma Prieta, California	USA	10/17/1989		He	+	4	Not given	Not given	7.1	60		1	Reimer, 1990
Coyote Lake, California	USA	8/6/1979		He	−		Not given	Not given	5.9	65		21	Reimer, 1990
Mt Diablo, California	USA	1/24/1980		He	−		Not given	Not given	5.5	155		35	Reimer, 1990
Salinas, California	USA	4/13/1980		He	−		Not given	Not given	4.9	35		28	Reimer, 1990
Livermore, California	USA	8/24/1980		He	+		Not given	Not given	4.1	120			Reimer, 1990
San Juan Bautista, California	USA	1/7/1981		He	−		Not given	Not given	4.5	45		10	Reimer, 1990
San Juan Bautista, California	USA	4/13/1980		D	−	7‰			4.8			1 month	O'Neil and King, 1980
Hollister, California (5 events)	USA	1979–1980		He	−				≥4.0			5–6 weeks	Reimer, 1980
Big Bear, California (swarm) (c)	USA	July 1979		Rn	+	72			4.8			60 ± 15	Craig, 1980
Big Bear, California (swarm) (c)	USA	July 1979		He	+	72			4.8			60 ± 15	Craig, 1980
Big Bear, California (swarm) (c)	USA	July 1979		CH_4	+	60			4.8			60 ± 15	Craig, 1980
Big Bear, California (swarm) (c)	USA	July 1979		Ar	+	25			4.8			60 ± 15	Craig, 1980
Big Bear, California (swarm) (c)	USA	July 1979		N_2	+	17			4.8			60 ± 15	Craig, 1980
Sand Point, Alaska	USA	2/14/1983		Rn	+	6–40 times background			6.3	180		6 weeks	Fleischer and Mogro-Campero, 1985
Mexico	Mexico	9/19/1985		Rn	+	200	Not given	Not given	8.1	260	nd	nd	Segovia et al., 1989
Reventador (d)	Ecuador	3/6/1987	14	Rn			Not given	Not given	6.9	367		50	Flores Humanante et al., 1990
	Ecuador				+	230	Not given	Not given	6.9	377		15–50	Flores Humanante et al., 1990
	Ecuador				+	400	Not given	Not given	6.9	339		15–35	Flores Humanante et al., 1990
	Ecuador				+	100	Not given	Not given	6.9	388		50	Flores Humanante et al., 1990
	Ecuador				+	100	Not given	Not given	6.9	183		15–40	Flores Humanante et al., 1990
	Ecuador				+	300	Not given	Not given	6.9	350		15–40	Flores Humanante et al., 1990
Ligurian Sea	France	5/1/1986		Rn	+	100	Not given	Not given	3.9	56	5	3	Borchiellini et al., 1991
Western Nagano	Japan	9/14/1984		N_2/Ar	−		Not given	Not given	6.8	50	230	120	Sugisaki and Sugiura, 1985, 1986
	Japan			He/Ar	−		Not given	Not given	6.8	50	230	120	Sugisaki and Sugiura, 1985, 1986
	Japan			CH_4/Ar	−		Not given	Not given	6.8	50	230	120	Sugisaki and Sugiura, 1985, 1986
Western Nagano	Japan	9/14/1984		H_2	−		Not given	Not given	6.8	50	120	50	Sugisaki and Sugiura, 1985, 1986
	Japan			H_2	+	2000	Not given	Not given	6.8	70		15	Sugisaki and Sugiura, 1985, 1986
?	Japan	8/6/1982		H_2			Not given	Not given	3.8	8.6		70	Sugisaki and Sugiura, 1985, 1986
Byakko	Japan	9/24/1990		He/Ar	+		Not given	Not given	6.6	280	0.1	coseismic	Nagamine and Sugisaki, 1991a
	Japan	10/16/1990		He/Ar	+		Not given	Not given	4.2	31	0.15	coseismic	Nagamine and Sugisaki, 1991a
	Japan	5/11/1991		He/Ar	+		Not given	Not given	3.9	35	0.25	coseismic	Nagamine and Sugisaki, 1991a
Chiba-Ken-Oki	Japan	6/1/1990		Rn	−	3	Not given	Not given	6	200	1		Wakita et al., 1989
Nagoya	Japan	4/3/1977		He/Ar	+		Not given	Not given	4.1	100	60	60	Sugisaki, 1978
	Japan	8/6/1977		He/Ar	+		Not given	Not given	4.3	15	60	50	Sugisaki, 1978
	Japan	8/15/1977		He/Ar	+		Not given	Not given	4.3	45	75	50	Sugisaki, 1978
	Japan	1/14/1978		He/Ar	+		Not given	Not given	7	216	130	120	Sugisaki, 1978
Izu–Oshima	Japan	1/14/1978		Rn	+	7	Not given	Not given	6.8	25	230		Wakita et al., 1988
Izu–Oshima	Japan	1/14/1978		Rn	−	8	Not given	Not given	6.8	25	7		Wakita et al., 1988
?	Japan	5/26/1983		H_2	+	100,000	Not given	Not given	7.7	480	?	?	Satake et al., 1985
Matsuyama area	Japan	12/10/1982		CH_4/Ar	+	120	Not given	Not given	4.9	50	120	100	Kawabe, 1984
Subducted zone	Japan	3/6/1984		Rn			Not given	Not given	7.9	1000	2	9	Igarashi and Wakita, 1990
	Japan	2/6/1987		Rn			Not given	Not given	6.7	130	4	3	Igarashi and Wakita, 1990
Kobe (e)	Japan	1/17/1995		Rn	+	200	Not given	Not given	7.2	30	90	75	Igarashi et al., 1995
	Japan	1/17/1995		Rn	+	1000	Not given	Not given	7.2	30	3	10	Igarashi et al., 1995
Pohai Bay	PR China	6/18/1969		Rn	+	60	Not given	Not given	7.4	170	170		Hauksson, 1981
Ningshin	PR China	8/5/1971		Rn	+	200	Not given	Not given	4.3	42	40		Hauksson, 1981
Hsingtang	PR China	6/6/1974		Rn	+	290	Not given	Not given	4.9	18	16		Hauksson, 1981
Haicheng	PR China	2/4/1975		Rn	+	38	Not given	Not given	7.3	50	270		Hauksson, 1981
Haicheng	PR China	2/4/1975		Rn	+	17	Not given	Not given	7.3	50	50		Hauksson, 1981
Haicheng	PR China	2/4/1975		Rn	−	43	Not given	Not given	7.3	140	66		Hauksson, 1981
Haicheng	PR China	2/4/1975		Rn	+	20	Not given	Not given	7.3	140	8		Hauksson, 1981
Haicheng	PR China	2/4/1975		Rn			Not given	Not given	7.3	26			Fleischer, 1980
	PR China						not given	Not given		14			Fleischer, 1981
Liaoyang	PR China						Not given	Not given	4.8	32			Fleischer, 1981

Tangshan	PR China	6/27/1976	Rn	+	15	Not given	Not given	7.8	50	970		Hauksson, 1981
Tangshan	PR China	6/27/1976	Rn	+	50	Not given	Not given	7.8	100	15		Hauksson, 1981
Tangshan	PR China	6/27/1976	Rn	−	40	Not given	Not given	7.8	130	1370		Hauksson, 1981
Tangshan	PR China	6/27/1976	Rn	+	27	Not given	Not given	7.8	130	162		Hauksson, 1981
Tangshan	PR China	6/27/1976	Rn			Not given	Not given	7.8	1800			Fleischer, 1981
Chienan	PR China	3/7/1977	Rn	+	70	Not given	Not given	6	200	3	1	Teng, 1980
Sabteh	PR China	4/8/1972	Rn	+	55	Not given	Not given	5.2	70	12		Teng, 1980
Takung	PR China	9/27/1972	Rn	+	34	Not given	Not given	5.8	54	12		Teng, 1980
Luhuo	PR China	2/6/1973	Rn	+	120	Not given	Not given	7.9	200	9		Wakita et al., 1988
Yiliang	PR China	4/22/1973	Rn	+	41	Not given	Not given	5.2	340	14		Teng, 1980
Songpan	PR China	5/8/1973	Rn	+	40	Not given	Not given	5.2	345	14		Hauksson, 1981
Mapien	PR China	6/29/1973	Rn	+	89	Not given	Not given	5.5	200	9		Wakita et al., 1988
Lungling	PR China	5/29/1976	Rn	+	20	Not given	Not given	7.5	20	510		Hauksson, 1981
Lungling	PR China	5/29/1976	Rn	+	15	Not given	Not given	7.5	190	425		Hauksson, 1981
Lungling	PR China	5/29/1976	Rn	+	8	Not given	Not given	7.5	210	160		Hauksson, 1981
Lungling	PR China	5/29/1976	Rn	+	12	Not given	Not given	7.5	215	130		Hauksson, 1981
Lungling	PR China	5/29/1976	Rn	+	7	Not given	Not given	7.5	360	75		Hauksson, 1981
Lungling	PR China	5/29/1976	Rn	+	20	Not given	Not given	7.5	420	290		Hauksson, 1981
Lungling	PR China	5/29/1976	Rn	+	200	Not given	Not given	7.5	450	12		Hauksson, 1981
Songpan-Pingwu	PR China	8/16/1976	Rn	+	29	Not given	Not given	7.2	40	480		Hauksson, 1981
Songpan-Pingwu	PR China	8/16/1976	Rn	+	11	Not given	Not given	7.2	100	420		Hauksson, 1981
Songpan-Pingwu	PR China	8/16/1976	Rn	+	20	Not given	Not given	7.2	100	190		Hauksson, 1981
Songpan-Pingwu	PR China	8/16/1976	Rn	+	70	Not given	Not given	7.2	320	1		Teng, 1980
Songpan-Pingwu	PR China	8/16/1976	Rn	−	12	Not given	Not given	7.2	320	200		Hauksson, 1981
Songpan-Pingwu	PR China	8/16/1976	Rn	+	90	Not given	Not given	7.2	340	48		Hauksson, 1981
Songpan-Pingwu	PR China	8/16/1976	Rn	−	60	Not given	Not given	7.2	340	160		Hauksson, 1981
Songpan-Pingwu	PR China	8/16/1976	Rn	+	55	Not given	Not given	7.2	390	160		Hauksson, 1981
Songpan-Pingwu	PR China	8/16/1976	Rn	+	110	Not given	Not given	7.2	560	34		Hauksson, 1981
Fengzhen	PR China	??/??/81	H_2	+	1000	Not given	Not given	5.8	285	15	7	Shi and Cai, 1986
Tangshan	PR China	7/27/1976	Rn	+	50	Not given	Not given	7.8	460	8	10	Shi and Cai, 1986
Ninghe	PR China	11/15/1976	H_2	+	900	Not given	Not given	6.9	nd	12	8	Jiang et al., 1981
Songpan	PR China	8/16/1976	Rn	+	100	Not given	Not given	7.2	350	1.5	10	Jiang and Li, 1981
Haicheng	PR China	1975	F−					7.4				Liang, 1980
Tangshan	PR China	1976	F−					7.8				Liang, 1980
Songpan-Pingwu	PR China	1976	F−					7.9				Liang, 1980
Ninghe	PR China	1977	F−					6.5				Liang, 1980
Taschkent	Ex-USSR	4/26/1966	Rn	+	20	Not given	Not given	5.3	5	400		Hauksson, 1981
Taschkent	Ex-USSR	3/24/1967	Rn	+	100	Not given	Not given	4	5	11		Hauksson, 1981
Taschkent	Ex-USSR	6/20/1967	Rn	+	23	Not given	Not given	3.5	5	3		Hauksson, 1981
Taschkent	Ex-USSR	7/22/1967	Rn	+	20	Not given	Not given	3.5	5	3		Hauksson, 1981
Taschkent	Ex-USSR	11/9/1967	Rn	+	23	Not given	Not given	3	5	8		Hauksson, 1981
Taschkent	Ex-USSR	11/17/1967	Rn	+	23	Not given	Not given	3.3	5	7		Hauksson, 1981
Taschkent	Ex-USSR	12/17/1967	Rn	+	23	Not given	Not given	3	5	4		Hauksson, 1981
Uzbekistan	Ex-USSR	2/13/1973	Rn	+	47	Not given	Not given	4.7	130	5		Hauksson, 1981
Markansu	Ex-USSR	8/11/1974	Rn	+	100	Not given	Not given	7.3	530	100		Hauksson, 1981
Tien Shan	Ex-USSR	2/12/1975	Rn	+	10	Not given	Not given	5.3	100	110		Hauksson, 1981
Gazli	Ex-USSR	5/17/1976	Rn	+	220	Not given	Not given	7.3	470	4		Hauksson, 1981
Gazli	Ex-USSR	5/17/1976	Rn	+	25	Not given	Not given	7.3	550	90		Hauksson, 1981
	Ex-USSR		Rn			not given	Not given	7	700			Fleischer, 1981
Gazli	Ex-USSR	5/17/1976	Rn			Not given	Not given	7.3	400			Fleischer, 1981
Isfarin-Batnen	Ex-USSR	1/31/1977	Rn	−	30	Not given	Not given	6.6	190	60		Hauksson, Fleischer, 1981
Isfarin-Batnen	Ex-USSR	1/31/1977	Rn	−	20	Not given	Not given	6.6	200	125		Hauksson, 1981
Alma-Ata	Ex-USSR	3/24/1978	Rn	+	32	Not given	Not given	7.1	65	50		Hauksson, 1981
Zaalai	Ex-USSR	11/1/1978	Rn	−	30	Not given	Not given	6.7	270	470		Hauksson, 1981
Zaalai	Ex-USSR	11/1/1978	Rn	−	40	Not given	Not given	6.7	300	470		Hauksson, 1981
Zaalai	Ex-USSR	11/1/1978	Rn	+	20	Not given	Not given	6.7	150	75		Hauksson, 1981
Zaalai	Ex-USSR	11/1/1978	Rn	−	20	Not given	Not given	6.7	150	70		Hauksson, 1981
Iran	Ex-USSR	9/16/1978	H_2S	+	170	Not given	Not given	?	nd	2	25	Barsukov et al., 1985
Duchambe	Ex-USSR	9/29/1981	Hg_{gas}	+	400	Not given	Not given	?	20		1.2	Varshal et al., 1985

(continued on next page)

Table 2 (*continued*)

Area (notes)	Country	Date	z [km]	Gas		δa [%]	Background level [cpm]	Signal level [cpm]	M	D [km]	d [days]	δt [days]	References
	Ex-USSR				+	9000	Not given	Not given	?			0.8	Varshal et al., 1985
Paravani, Caucasus	USSR	5/13/1986							5.6				Bella et al., 1995a,b
Spitak, Caucasus	USSR	12/7/1988							6.9				Bella et al., 1995a,b
Kamchatka Peninsula	Russia	3/2/1992	34	Na^+, Ca^{2+}, HCO_3,SO_4^{2}	+	Exceeds 3σ level				100		35	Biagi et al., 2000a,b
				Ca^{2+}	+								
				HCO_3^-	−								
				SO_4^{2-}	+								
Kamchatka Peninsula	Russia	11/13/1993	56	Na^+, Ca^{2+}, HCO_3,SO_4^{2}	+	Exceeds 3σ level				152		6–80	Biagi et al., 2000a,b
				Ca^{2+}	+								
				HCO_3^-	−								
				SO_4^{2-}	+								
Kamchatka Peninsula	Russia	1/1/1996	10	Na^+, Ca^{2+}, $HCO_3SO_4^{2}$	+	Exceeds 3σ level				96		107	Biagi et al., 2000a,b
				Ca^{2+}	+								
				HCO_3^-	−								
				SO_4^{2-}	+								
Kamchatka Peninsula	Russia	6/21/1996	1	Na^+, Ca^{2+}, HCO_3,SO_4^{2}	+	Exceeds 3σ level				228		72	Biagi et al., 2000a,b
				Ca^{2+}	+								
				HCO_3^-	−								
				SO_4^{2-}	+								
Kamchatka Peninsula	Russia	12/5/1997	10	Ar	+	Exceeds 3σ level				366		6–80	Biagi et al., 2000a,b
				N_2	+								
Irpinia	Italy	11/23/1980		Rn	+	25	Not given	Not given	6.5	220	150	150	Allegri et al., 1983
Irpinia	Italy	11/23/1980		Rn	+	170	Not given	Not given	6.5	200	180	180	Allegri et al., 1983
Northern Taiwan	Taiwan	10/18/1980	8.2	Rn	nd		Not given	Not given	5.8	39	nd	19	Liu et al., 1985
	Taiwan	5/14/1981	8.2	Rn	nd		Not given	Not given	5.2	23	nd	11	Liu et al., 1985
	Taiwan	6/21/1981	8.4	Rn	nd		Not given	Not given	4.6	14	nd	15	Liu et al., 1985
	Taiwan	7/18/1981	6.7	Rn	nd		Not given	Not given	5	37	nd	4	Liu et al., 1985
	Taiwan	10/31/1982	9.8	Rn	nd		Not given	Not given	5.3	45	nd	51	Liu et al., 1985
	Taiwan	11/??/1982		Rn	+	3–4 times background			4.1	60		2 weeks	Liu et al., 1983
Uttarkashi (f)	India	10/20/1991		Rn	+	200	Not given	Not given	7	450	7	15	Virk and Baljinder, 1994
	India				+	300	Not given	Not given	7	270	7	15	Virk and Baljinder, 1994
	India				+	180	Not given	Not given	7	330	7	3	Virk and Baljinder, 1994
Himachal Pradesh (g)	India	4/9/1992		Rn	+	195	Not given	Not given	2.2	166		2	Virk and Baljinder, 1995
	India	5/23/1995		Rn	+	165	Not given	Not given	2.7	105		3	Virk and Baljinder, 1995
	India	1/12/1993		Rn	+	153	Not given	Not given	4.4	440		9	Virk and Baljinder, 1995
	India	1/12/1993		Rn	+	183	Not given	Not given	4.4	440		9	Virk and Baljinder, 1995
	India	7/21/1992		Rn	+	250	Not given	Not given	3.6	265		13	Virk and Baljinder, 1995
	India	8/5/1993		Rn	+	242	Not given	Not given	3.7	325		10	Virk and Baljinder, 1995
	India	8/5/1993		Rn	+	227	Not given	Not given	3.7	325		10	Virk and Baljinder, 1995
Maheshwaram	India	4/17/2002		Rn	+	100	Not given	Not given	<1	30	<1		Reddy et al., 2004
Chamoli (groundwater)	India	3/29/1999		Rn	+	69.66 Bq/l	56.69 Bq/l	Not given	6.8			2	Virk et al., 2001
Chamoli (soil gas)	India	3/29/1999		Rn	+	46.63 Bq/l	24.31 Bq/l	Not given	6.8			2	Virk et al., 2001
Chamoli	India	3/29/1999		He	+	5.6 ppm	5.1 ppm	Not given	6.8			5	Virk et al., 2001

		Jan 1991				background							
Chiba-ken Toho-oki	Japan	6/1/1990	59	Rn	−	5	2350	2225	6	200	2	2	Wakita et al., 1991
Fukushima	Japan	Jan 1987		Rn	−	2	2025	1975	6.6	260	0	0	Igarashi et al., 1990
Fukushima	Japan	Feb 1987		Rn	−	11	2025	1800	6.7	130	0	0	Igarashi et al., 1990
Fukushima	Japan	Apr 1987		Rn	−	9	2000	1825	6.6	110	0	0	Igarashi et al., 1990
Kobe	Japan	1/17/1995	14	Cl^-	+	10	13.85 ppm	15.3 ppm	7.2	20	4		Tsunogai & Wakita, 1995; Tsunogai & Wakita, 1996
Kobe	Japan	1/17/1995		Rn	−	5	3100	2950	7.2	260			Ohno & Wakita, 1996
Western Nagano prefecture	Japan	9/14/1984		Rn	+					65		2 weeks	Ui et al., 1988
Eastern Pyrenees	France	2/18/1996	7.7	Cl^-	+	36	0.272 mml/l	0.369 mml/l	5.2	29	5	10 to 13	Toutain et al., 1997
Hyogo-Ken Nambu Zisin	Japan	Sep 1984		He/Ar	−	25	0.112***	0.084***	6.9	50			Sugisaki et al., 1996
Hyogo-Ken Nambu Zisin	Japan	Sep 1984		N_2/Ar	−	10	126***	113***	6.9	50			Sugisaki et al., 1996
Hyogo-Ken Nambu Zisin	Japan	Sep 1984		CH_4/Ar	−	32	22***	15***	6.9	50			Sugisaki et al., 1996
Hyogo-Ken Nambu Zisin	Japan	Jan 1995		He/Ar	−	4	0.113***	0.109***	7.2	220	3 h	15 min	Sugisaki et al., 1996
Izu–Oshima–kinkai	Japan	1/14/1978	7.0	Rn	+	15%			7.0	25		5	Wakita et al., 1980
Hyogo-Ken Nambu Zisin	Japan	Jan 1995		N_2/Ar	−	2	132***	130***	7.2	220	3 h	15 min	Sugisaki et al., 1996
Hyogo-Ken Nambu Zisin	Japan	Jan 1995		CH_4/Ar	−	6	21.8***	20.6***	7.2	220	3 h	15 min	Sugisaki et al., 1996
Mindoro	Philippines	11/14/1994		Rn	+	600	Not given	Not given	7.1	48	7	22	Richon et al., 2003
Perpignan	France	1996		HCO_3^-	+	135 mg/L	80–110 mg/l		5.2	100			Perez, 1996
Perpignan	France	1996		Ca^{2+}	+	45 mg/l	20–30 mg/l		5.2	100			Perez, 1996
Perpignan	France	1996		Cl^-	+	75 mg/l	35 mg/l		5.2	100			Perez, 1996
Galicia	Spain	2 events, 11/29/1995 12/24/1995		Cl^-	+	26 mg/l	24 mg/l		4.64.6	90			Redondo et al., 1996
Galicia	Spain	2 events, 11/29/1995 12/24/1995		Br^-	+				4.6	90			Redondo et al., 1996
Galicia	Spain	2 events, 11/29/1995 12/24/1995		δD	+				4.6	90			Redondo et al., 1996

Note: The data through the earthquakes at Himachal Pradesh have been adapted from a table by Toutain and Baubron (1999).
Legend:
z = epicentral depth.
δa = deviation.
M = magnitude.
D = epicentral distance.
d = duration.
δt = days before event.
+, gas emission increase.
−, gas emission decrease.
*** unitless (ratio).
a Values from Hauksson (1981). This author does not supply time lag values.
b Hydrogen values from Sato et al. (1986). H_2 displays a very complex pattern probably linked to a sudden increase in seismicity (11 events of magnitude 5.2 to 6.7 within 6 months).
c The Big Bear earthquake swarm occurred on June 29 and 30. The main shock was $M = 4.8$ and was considered as the total event.
d Time lags vary at some sites which have several probes. No duration of anomalies is shown because of the track-etch method used.
Values of deviation of signal at each site are from one of the several probes. Values at one site (epicentral distance of 350 km) are either positive or negative, depending on the probe (Flores Humanante et al., 1990).
e According to data by Igarashi et al. (1995), we can assume the existence of two precursors, one lasting about 3 months and the other being a spike-like one occurring 7 days before the onset.
f Magnitudes were indicated to be 6.5 (Mb) and 7.0 (MS).
g Only anomalies above la have been selected. Graphical data are not enough precise to estimate values of duration and time lags of claimed anomalies.
Note: These notes are from the original table compiled by Toutain and Baubron (1999).

of positively and negatively charged particles, and an electric field is generated. In the rock samples, the near field E_s is related to the dipole moment p by

$$E_s = \frac{1}{4\pi\varepsilon_0}\frac{p}{r^3}, \tag{9}$$

where r is the distance between the dipole and the antenna and ε_0 is the permittivity of free space. For earthquakes, Ogawa et al. (1985) propose that the electric fields actually generated are the induced field E_i in the VLF frequency range and the radiation field E_r for the LF frequency range. These fields are related to the dipole moment by

$$E_i = \frac{1}{4\pi\varepsilon_0}\frac{\dot{p}}{cr^2}, \tag{10}$$

and

$$E_r = \frac{1}{4\pi\varepsilon_0}\frac{\ddot{p}}{c^2 r}, \tag{11}$$

where c is the velocity of light and the dots represent derivatives with respect to time.

Pierce (1976) presented a model that relates changes in atmospheric electricity to the emission of radon gas from the earth. The radon gas alters certain parameters that affect atmospheric electricity, including fair-weather conductivity near the ground and the electric field (i.e., potential gradient). Specifically, the model predicts that the conductivity near the ground would increase by about 50%, while the electric field would decrease by about 30%.

4.5. Gas emission observations

In the late 1960s and early 1970s reports primarily from Russia and China indicated that concentrations of radon gas in the earth apparently changed prior to the occurrences of nearby earthquakes (Lomnitz, 1994). This stimulated a number of experiments in other parts of the world to monitor underground radon with time and to look for radon changes associated with earthquakes. Since radon is a radioactive gas, it is easy and relatively inexpensive to monitor instrumentally, and its short half-life (3.8 days) means that short-term changes in the radon concentrations in the earth can be monitored with very good time resolution. While other gases have also been looked at as possible earthquake precursors, the bulk of the experiments reported in the scientific literature have focused on radon.

In our literature survey, we found reports of 159 observations of changes in gas emissions from 107 earthquakes. Of these, there were 125 radon observations from 86 earthquakes, 7 observations of hydrogen gas from 7 earthquakes, 7 observations of helium gas from 7 earthquakes, 10 observations of helium/argon gas ratios from 10 earthquakes, 4 observations of methane/argon ratios from 4 earthquakes, 3 observations of nitrogen/argon ratios from 3 earthquakes, 2 observations of chlorine ions from 2 earthquakes, and 1 observation of mercury gas from 1 earthquake. There are also reports of possible changes in the emission of other gases, such as carbon monoxide and carbon dioxide, from the earth associated with earthquakes, but no specific measurements were reported in the papers we surveyed.

Table 2 contains the complete listing of gas emission anomalies found in our literature search along with estimates of the initiation time, strength and duration of the gas anomalies. Because the preponderance of data is concerned with radon gas changes, we summarize those results here.

There is a very wide range of earthquake magnitudes for which anomalous radon precursors have been reported. In the dataset in Table 2 the smallest earthquake magnitude is 1.5 and the largest is 7.9. Most of the observations are for earthquakes greater than magnitude 4.0. Radon gas changes up to 1200% relative to background radon concentration levels are reported in Table 2 although most of the changes are between 20% and 200%, with the most common reported change between 50% and 100% (Fig. 1). In Table 2, 83% of the observations reported that radon levels increased prior to the earthquake relative to the background radon levels.

In Fig. 2 the times of initiation of the radon anomalies and the durations of the radon anomalies are shown. Most of the radon anomalies began within 30 days of the earthquake, and most lasted less than 200 days. In some cases in Table 3 the radon anomaly initiated and terminated before the earthquake (δt greater than d in the Table 3), while in other cases the radon anomaly continued after the time of the earthquake (δt less than d in the Table 3). Thus, there does not appear to be any diagnostic behavior of either the beginning or the end of a radon anomaly that gives a consistent clue about when an earthquake is to happen. The best that can be said is that most of the time the earthquake takes places within a month of the time that an increase in radon gas is observed.

Fig. 3 shows the dependence of the magnitude of the reported radon anomalies on distance of the observation site to the earthquake epicenter and on the magnitude of the event. The greatest anomalies are reported closest to the epicenters of the coming earthquakes, suggesting that the

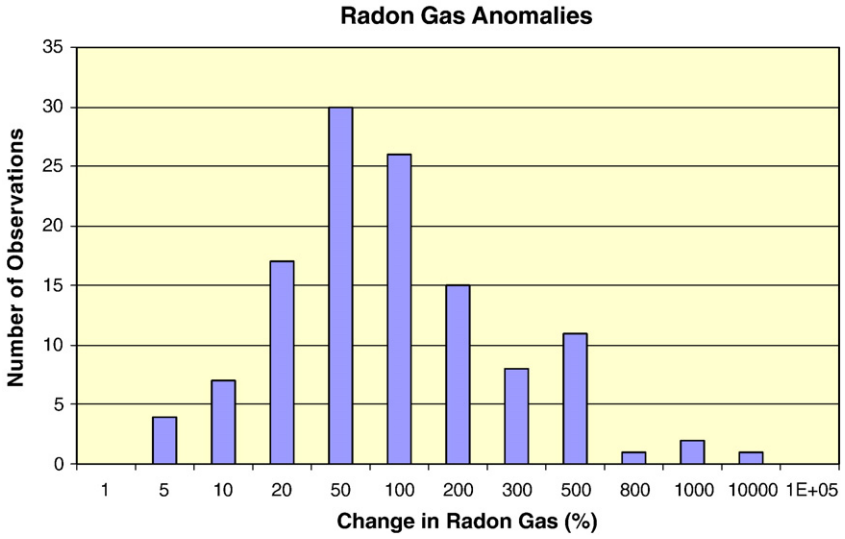

Fig. 1. Distribution of reported maximum changes in radon gas concentrations in the earth (in percent relative to the background radon levels) prior to earthquakes. Most of the changes are between 20% and 200%. The vertical axis represents the number of observations for each data range.

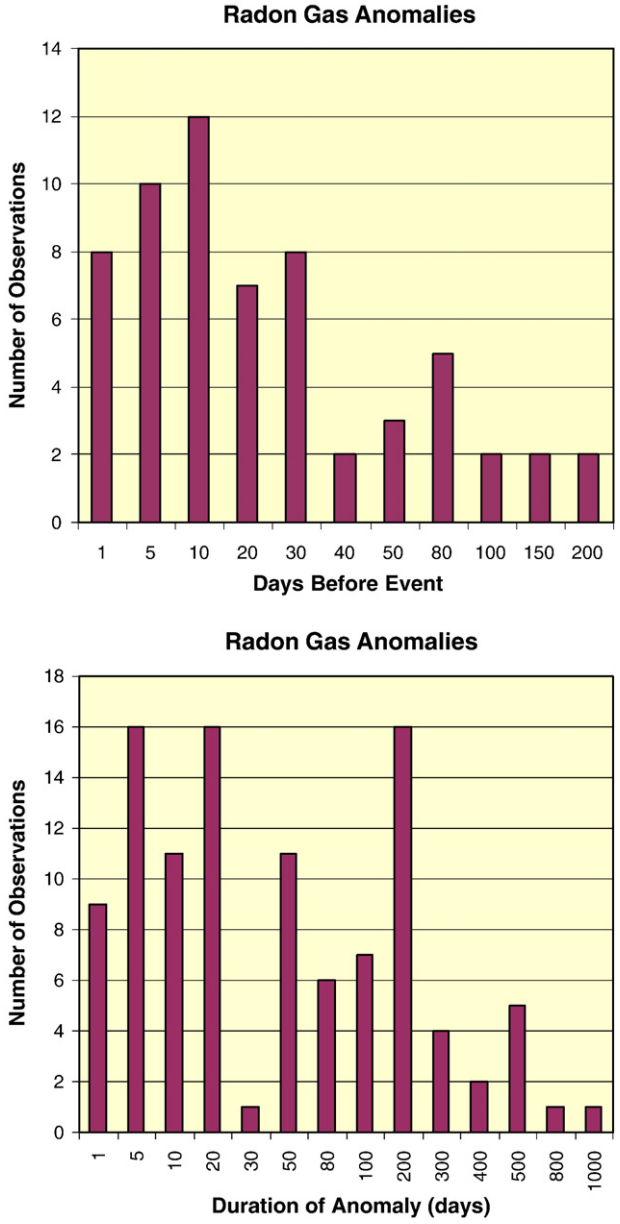

Fig. 2. Distribution of reported times of initiation of the radon anomaly prior to the earthquake (top) and of the durations of the radon anomaly (bottom). Most of the radon anomalies began within 30 days of the earthquake and lasted less than 200 days.

radon anomalies are associated with some physical processes in or near the earthquake fault zone. On the other hand, the amplitude of the radon anomaly does not seem to depend on the magnitude of the coming earthquake. This appears to indicate that whatever causes the anomalous radon emissions does not control the size of the earthquake. The significant amount of scatter in the data precludes the determination of any useful regression curves of radon anomaly as a function of either distance or magnitude. On the other hand, curves that represent the possible extremal values from the data in Table 3 are plotted in Fig. 3, and the corresponding equations. for these lines are summarized in Table 4. These curves are intended to place a possible upper bound on the expected anomaly radon values as a function of magnitude and distance as determined by the data collected in this study.

Fig. 4 analyzes the dependence of magnitude of the coming even with the start time of the radon anomaly relative to the time of the earthquake and with the duration of the anomaly. Greater times between the start of the anomaly and the earthquake as well as longer durations of the radon anomalies appear to be associated with larger event magnitudes. Thus, in an earthquake prediction scheme, the longer the duration of a radon anomaly, the larger the earthquake that might be expected. Again, line segments representing possible extremal values of the data as a function of magnitude are plotted in Fig. 4.

The paucity of data for the other types of gases in Table 2 precludes analyses similar to those of Figs. 1–4. However, some general statements can be made about the observational data for these other gases. First, for the other gases the distribution of reported anomaly amplitudes, time durations, time of initiation before the event, and distance to the epicenter appear in all cases to be similar to the observations for radon gas. The amplitudes of the anomalies seem to vary from gas to gas, with the largest reported increase being 100,000% for an observation of H_2 prior to an earthquake. This would seem to suggest that other gases besides radon may give higher amplitude gas emissions prior to earthquakes if they were widely monitored. Finally, while radon tends to increase in emission before earthquakes, this appears to be true of some but not all of the gases in Table 2. Of these other gases for which data were collected, H_2 (6 of 7 observations), He/Ar (7 of 10 observations) and Cl^- (2 of 2 observations) show gas increases before the earthquakes, while He (4 of 7 observations), CH_4/Ar (3 of 4 observations) and N_2/Ar (3 of 3 observations) report gas decreases before the earthquakes.

4.6. Gas emission models

Thomas (1988) provides a summary of physical processes proposed to explain geochemical precursors, including gas emissions, to earthquakes. Although many different models have been proposed in the literature to account for the various observed geochemical precursors, most can be associated with one of the following mechanisms:

- Physical and/or chemical release by ultrasonic vibration (UV model);
- Chemical release due to pressure sensitive solubility (PSS model);
- Physical release by pore collapse (PC model);
- Chemical release by increased loss or reaction with freshly created rock surfaces (IRSA model);
- Physical mixing due to aquifer breaching and/or fluid mixing (AB/FM model).

These mechanisms are briefly described below. Readers are referred to the review paper of Thomas (1988) for the original references.

4.7. Ultrasonic vibration model

This model proposes that loosely-bound constituents in subsurface rocks can be released by ultrasonic vibration. Laboratory studies have indicated that rocks react more readily with water when ultrasonic vibration is applied. Field studies have also shown that geochemical anomalies can be generated in response to a subsurface explosive discharge, similar to those commonly used in seismic exploration.

Critics of this model contend that the relatively high frequencies necessary to release chemical species from subsurface rocks are either too weak or completely absent in the frequency spectrum of earthquakes. In addition, geochemical anomalies associated with explosions are typically much smaller that those associated with earthquakes. Also, these explosion-induced anomalies occur some time after the explosion itself, indicating that some other mechanism may be generating these anomalies.

4.8. Pressure sensitive solubility model

This model proposes that increases in dissolved chemical species in groundwater are caused by increases in fluid pressure due to precursory stress changes. This mechanism is unlikely to contribute significantly to the generation of geochemical anomalies, because the required stress changes are on the order of tens to hundreds of bars. Even though stress changes of this order are common in earthquakes,

Table 3
Reported precursory groundwater level changes associated with earthquakes.

Earthquakes with reported groundwater precursors								
Earthquake	Mag.	Date	*D* [km]	*A* [m]	*T* [day]	*t* [day]	Reference	Notes
Turkmenia, former U.S.S.R.	7.3	10/5/1948	10	−1.300	180.0	7.0	Mil'kis, 1984	*
Turkmenia, former U.S.S.R.	7.3	10/5/1948	10	−0.800	60.0	45.0	Mil'kis, 1984	*
Turkmenia, former U.S.S.R.	7.3	10/5/1948	90	−0.400	225.0	40.0	Mil'kis, 1984	*
Turkmenia, former U.S.S.R.	7.3	10/5/1948	90	−0.600	225.0	40.0	Mil'kis, 1984	*
Turkmenia, former U.S.S.R.	7.3	10/5/1948	90	−0.400	225.0	40.0	Mil'kis, 1984	*
Turkmenia, former U.S.S.R.	7.3	10/5/1948	90	+/−0.5	150.0	70.0	Mil'kis, 1984	*
Uzbekistan, former U.S.S.R.	7.3	5/17/1976	200	−2.000	1.0	0.5	Ishankulov and Kalugin, 1976	*
Uzbekistan, former U.S.S.R.	7.3	5/17/1976	530	−16.000	300.0	40.0	Mil'kis and Voronin, 1983	*
Tadzhikistan, former U.S.S.R.	6.3	1/31/1977	210	1.000	135.0	—	Sultankhodzhaev and Chernov, 1978	*
Turkmenia, former U.S.S.R.	4.5	3/25/1977	120	−0.080	60.0	25.0	Zhukov et al., 1978	*
Tadzhikistan, former U.S.S.R.	5.0	12/6/1977	25	2.000	150.0	—	Sultankhodzhaev and Chernov, 1978	*
Kirgizia, former U.S.S.R.	6.6	3/25/1978	300	−0.500	35.0	20.0	Orolbaev, 1984	*
Kirgizia, former U.S.S.R.	6.6	3/25/1978	140	−0.200	14.0	10.0	Orolbaev, 1984	*
Kirgizia, former U.S.S.R.	6.8	11/2/1978	140	−0.800	3.0	1.0	Mavlyanov and Sultankhodzhaev, 1981	*
Uzbekistan, former U.S.S.R.	5.1	12/11/1980	150	−0.110	40.0	30.0	Kissin et al., 1984a	*
Uzbekistan, former U.S.S.R.	5.1	12/11/1980	150	−0.005	5.0	5.0	Kissin et al., 1984a	*
Uzbekistan, former U.S.S.R.	5.1	12/11/1980	160	−0.030	1.0	0.5	Kissin et al., 1984a	*
Kazakhstan, former U.S.S.R.	5.3	12/31/1982	95	0.130	2.0	—	Ospanov and Mizev, 1985	*
Tadzhikistan, former U.S.S.R.	5.9	12/26/1984	100	8.100	3.0	—	Sultankhodzhaev et al., 1986	*
Kuril Islands, former U.S.S.R.	7.5	3/22/1978	270	−0.030	7.0	2.5	Monakhov, 1981	*
Kuril Islands, former U.S.S.R.	7.0	6/21/1978	450	−0.045	6.0	3.0	Monakhov et al., 1980	*
Kuril Islands, former U.S.S.R.	5.2	10/11/1978	90	−0.070	6.0	2.0	Monakhov et al., 1980	*
Kuril Islands, former U.S.S.R.	5.6	12/2/1978	440	−0.090	9.0	2.0	Monakhov et al., 1979	*
Kuril Islands, former U.S.S.R.	5.4	2/25/1979	95	−0.040	5.0	1.5	Monakhov, 1981	*
Kuril Islands, former U.S.S.R.	6.3	2/15/1980	170	−0.030	6.0	2.0	Monakhov, 1981	*
Baykal area, former U.S.S.R.	5.0	10/2/1980	25	−0.300	60.0	—	Golenetskii et al., 1982	*
Lutt Plateau, Iran	6.7	1/16/1979	400	−0.350	21.0	14.0	Mil'kis & Voronin, 1983	*
Hindu Kush, Afghanistan	6.6	5/2/1981	450	0.015	4.0	3.0	Kissin et al., 1984b	*
Singhai, China	6.8	3/24/1971	20	−0.300	20.0	7.0	Wang et al., 1984a	*
Singhai, China	6.8	3/24/1971	—	−0.410	30.0	1.0	Hamilton, 1975	*
Liaoning, China	7.3	2/4/1975	40	−0.100	8.0	5.0	Raleigh et al., 1977	*
Liaoning, China	7.3	2/4/1975	145	−0.030	4.0	2.0	Raleigh et al., 1977	*
Hebei, China	7.8	7/28/1976	5	−15.000	2640.0	5.0	Wang et al., 1984b	*
Hebei, China	7.8	11/15/1976	30	−13.000	1090.0	5.0	Wang et al., 1984b	*
Hebei, China	6.9	11/15/1976	100	−3.000	100.0	30.0	Alimova and Zubkov, 1983	*
Liaoning, China	5.6	11/27/1977	20	−0.500	1.2	—	Wang et al., 1984a	*
Liaoning, China	5.6	11/27/1977	20	−0.580	—	0.4	Cai and Shi, 1980	*
near Izu Peninsula, Japan	7.0	1/14/1978	35	+/−2.0	288.5	30.0	Alimova and Zubkov, 1983	*
Izu Peninsula, Japan	6.6	6/29/1980	30	0.480	40.0	15.0	Yamaguchi, 1980	*
California, U.S.A.	5.0	2/24/1972	—	−0.050	25.0	10.0	Kovach et al., 1975	*
California, U.S.A.	4.7	4/9/1972	—	−0.100	40.0	15.0	Kovach et al., 1975	*
San Jacinto, California, U.S.A.	5.5	2/25/1980	35	0.450	3.7	3.4	Merifield and Lamar, 1981	*
Kettleman Hills, California, U.S.A (2 wells)	6.1	8/4/1985	35	+3.0 cm, +3.8 cm		3	Roeloffs and Quilty, 1997	
Taiwan	6.3	12/29/1984	—	0.050	0.0	0.0	Yu and Mitchell, 1988	
Taiwan	6.3	6/12/1985	—	0.030	0.0	0.1	Yu and Mitchell, 1988	
Taiwan	6.2	1/16/1986	—	0.240	0.0	0.0	Yu and Mitchell, 1988	
Izu–Oshima–kinkai, Japan	7.0	1/14/1978	30	−0.300	0.0		Wakita, 1984	
southwest Japan	6.6	3/18/1987	226	0.2 ml/s	15 min	0	Kawabe et al., 1988	
Tokyo Bay, Japan	5.9	2/2/1992	90–110	0.040	2.0	1.5	Igarashi et al., 1992	
Tokyo Bay, Japan	5.9	2/2/1992	90–110	0.034	2.0	1.5	Igarashi et al., 1992	
Tokyo Bay, Japan	5.9	2/2/1992	90–110	−0.100	1.0	0.5	Igarashi et al., 1992	
Tokyo Bay, Japan	5.9	2/2/1992	90–110	0.200	0.0		Igarashi et al., 1992	
Tokyo Bay, Japan	5.9	2/2/1992	90–110	−0.038	0.0		Igarashi et al., 1992	
Tokyo Bay, Japan	5.9	2/2/1992	90–110	0.010	0.0	1.0	Igarashi et al., 1992	
Hokkaido, Japan	8.1	10/4/1994	1260	−50 cm		10	Igarashi et al., 1996	
Sanriku, Japan	7.8	12/28/1994	800	−50 cm		10	Igarashi et al., 1996	
Izu Peninsula, Japan (6 swarms, >1000 events/day)	≥2.5	9/1995–10/1995,10/1996, 3/1997, 4/1998–5/1998, 5/2002, 6/2002	30	0.0024 m/h	<1 day	<1	Koizumi et al., 1999, Koizumi et al., 2004	
Tono Mine, Japan	6.1	9/24/1990	510	0.5	5 days	0	King et al., 2000	
Tono Mine, Japan	7.2	10/4/1994	220	0.5	10 days	0	King et al., 2000	
Tono Mine, Japan	7.5	12/28/1994	800	0.5	10 days	0	King et al., 2000	
Tono Mine, Japan	8.1	1/17/1995	1260	0.5	30 days	0	King et al., 2000	
Tono Mine, Japan	6.6	9/5/1996	290	0.2	5 days	0	King et al., 2000	
Tono Mine, Japan	5.8	3/16/1997	50	2	6 months	0	King et al., 2000	
Koyna-Warna, western India	4.4	4/25/1997	3	+3 cm, +7 cm (2 wells)	23 days	23	Chadha et al., 2003	
Koyna-Warna, western India	4.3	2/11/1998	12	+5 cm	3 days	3	Chadha et al., 2003	
Koyna-Warna, western India	4.7	4/6/2000	24	+2.5 cm	28 days	28	Chadha et al., 2003	
Koyna-Warna, western India	5.2	9/5/2000	12–20	−(0.4–8) cm (7 wells)	24–28 days	24–28	Chadha et al., 2003	
Thessaloniki, Greece	4.8	10/20/1988	33–46	5–10 cm	5 days	5	Asteriadis and Livieratos, 1989	

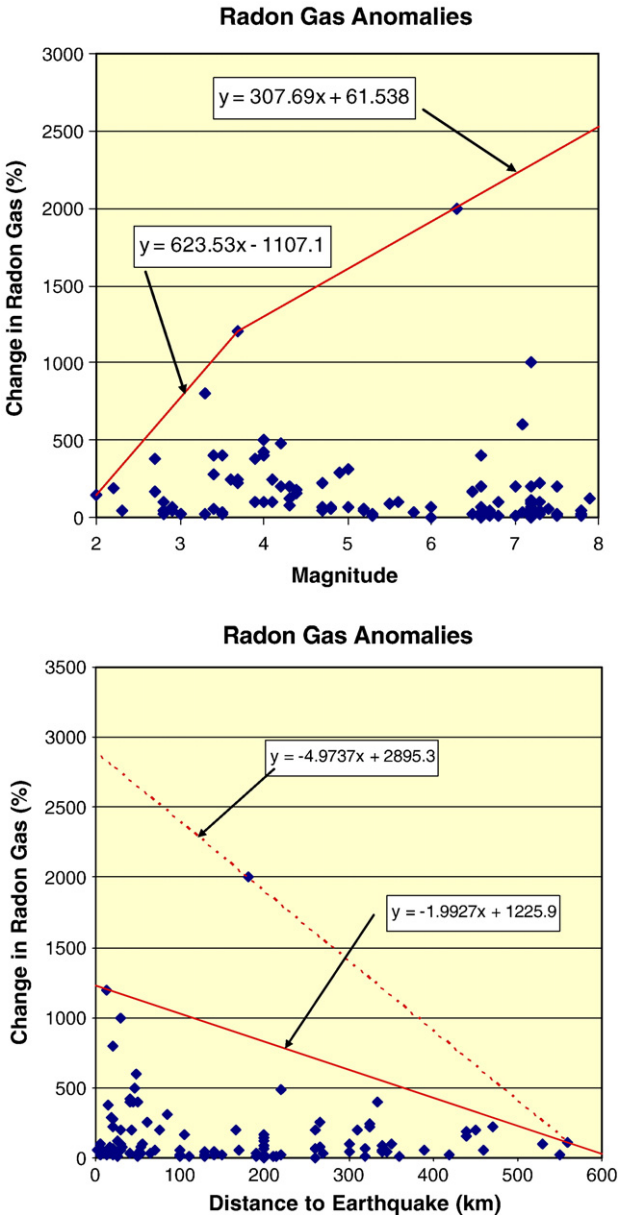

Fig. 3. Distribution of reported changes in radon gas concentrations with distance to the earthquake (top) with event magnitude (bottom). The greatest anomalies are reported closest to the epicenters, but no dependence on magnitude is seen. Curves representing the possible extremal values of the data sets are also shown. On the bottom figure, two different extremal lines are shown, where the solid line ignores the one extreme data point at about 180 km epicentral distance.

there is little evidence that these stress changes are transferred to the fluid phase in the rocks.

4.9. Pore collapse model

This model suggests that, as stresses in the earth increase prior to an earthquake, the pore volume in the rocks collapses, thereby releasing chemical species into the groundwater, generating a geochemical anomaly. Decreases in rock pore volume have been demonstrated in a number of laboratory and field studies.

The importance of the pore collapse model to the study of earthquake precursors is not well established. Laboratory studies indicate that volume losses in rocks tend to occur at relatively low stress levels and tend to be small. In fact, high stresses in porous rocks result in an increase in pore volume for most rocks. Also, decrease in pore volume is an irreversible process and would not account for the repeated and cyclic nature of precursory geochemical precursors.

4.10. Increased reactive surface area model

For this model, it is proposed that microfracturing prior to major earthquakes leads to increases in ion and gas concentrations in the groundwater. The fracturing process has two effects. The first is that it allows trapped gases to escape from the rock matrix. The second is that it produces fresh silicate surfaces, which are believed to increase the rate of reaction with groundwater.

Laboratory studies indicate that microfracturing and the associated dilatancy can increase the porosity of rocks appreciably, from 20% up to as much as 400%. Reaction with fresh rock surfaces has been shown to significantly increase ions in groundwater. Also, laboratory studies have indicated that the release of gases, most notably radon, can increase substantially at the stress levels associated with microfracturing (Holub and Brady, 1981). Field studies have indicated a correlation with increased radon concentrations in groundwater and regional stress and deformation changes.

The major uncertainty associated with this model is the fact that laboratory studies have indicated that rock dilatancy and the associated increases in pore volume only become important in rocks near the failure strength. This would indicate that the mechanism should be confined to a small volume of rock close to the fault. This is in conflict with the observations of geochemical precursors at significant distances from seismogenic faults. However, it has been argued that this model does not consider the importance of stress corrosion cracking and subcritical crack growth, which can occur at relatively low stress levels and high moisture content.

4.11. Aquifer breaching/fluid mixing model

This model can be used to account for anomalous changes in groundwater geochemistry as the result of mixing of chemical species from two distinct aquifer systems. The advantage of this model is that it can account for both increases and decreases in chemical species and gas concentrations, as well as the concurrent temperature changes that often accompany these geochemical precursors.

The mechanism of fluid mixing is believed to be due to precursory fracturing of hydrologic barriers that separate the individual aquifer systems. A similar mechanism has been proposed by Byerlee (1993) to explain the compartmentalization of high-pressure fluid regions in the vicinity of faults. This mechanism was cited by Fenoglio et al. (1994a,b; 1995) to support their conclusion that the electrokinetic mechanism is the process by which transient ULF magnetic field precursors were generated prior to the Loma Prieta earthquake.

4.12. Groundwater level change observations

Changes in groundwater level changes prior to earthquakes have been reported back to early historic times (Martinelli, 2000). This is

Notes to Table 3:
*Compiled by Kissin and Grinevsky, 1990.
D = epicentral distance.
A = amplitude (+, groundwater rise; −, groundwater drop).
T = time (period of time from the beginning of the precursor to the earthquake origin time).
t = extremum time (period of time from the onset of a precursor extremum to the earthquake origin time).

Table 4
Summary of equations for extremal value curves.

Figure number	Type of anomaly	Physical quantity (y vs. x)	Equation
3	Radon gas	Change in radon gas vs. magnitude	$y = 307.69x + 61.538$
3	Radon gas	Change in radon gas vs. magnitude	$y = 623.53x - 1107.1$
3	Radon gas	Change in radon gas vs. distance to earthquake	$y = -4.9737x + 2895.3$
3	Radon gas	Change in radon gas vs. distance to earthquake	$y = -1.9927x + 1225.9$
4	Radon gas	Anomaly duration vs. magnitude	$y = 359.72x - 1005.8$
4	Radon gas	Anomaly duration vs. magnitude	$y = 135.59x - 71.186$
4	Radon gas	Days before event vs. magnitude	$y = 42.857x - 85.714$
7	Water level change	Water level change vs. distance to earthquake	$y = -0.9867\mathrm{Ln}(x) + 7.5439$
7	Water level change	Water level change vs. distance to earthquake	$y = 0.9867\mathrm{Ln}(x) - 7.5439$
7	Water level change	Water level anomaly vs. magnitude	$y = 4.2632x - 17.053$
7	Water level change	Water level anomaly vs. magnitude	$y = -4.2632x + 17.053$
8	Water level change	Time of anomaly maximum before event vs. magnitude	$y = 16.207x - 48.31$
8	Water level change	Time of anomaly maximum before event vs. magnitude	$y = 57.5x - 230$
8	Water level change	Start of anomaly before event vs. magnitude	$y = 69.25x - 196.25$
8	Water level change	Start of anomaly before event vs. magnitude	$y = 150x - 600$

not surprising, because water is essential to human life and the use of wells to provide water for human settlements has been important going back to the beginning of human civilization. Any unusual changes in groundwater levels, particularly dug wells that either drop significantly in level or even go dry, would be noted and be a cause for concern. Unfortunately, most such reports are anecdotal rather than of a careful scientific measurement, and so they would not be reflected in the database accumulated in this study.

The groundwater change observations are summarized in Table 3. There are 52 observations from 32 earthquakes, with the earthquake magnitudes ranging up to 7.8. Most of the reports come from within 200 km of the epicenter of the earthquake, with the greatest distance for an observation being 530 km.

Fig. 5 shows the distribution of the maximum water level changes reported prior to the earthquakes in Table 3. While the maximum changes ranged from a 15 m drop in water level to an 8 m rise, most of the changes were less than 1 m. In 72% of the cases, the groundwater level was observed to drop before the earthquake. Fig. 6 indicates that most of the changes in groundwater levels began within about a year of the coming earthquake, but some much earlier than that. However, generally the greatest change in groundwater level was observed within about 40 days of the coming earthquake.

Fig. 7 shows the dependence of the amplitude of the groundwater level change with distance to the earthquake epicenter and with magnitude of the coming earthquake. Fig. 8 illustrates the start time of the groundwater anomaly and the time of the greatest anomaly as a function of the magnitude of the coming earthquake. While there are not as many data points as for the radon data, the tendencies in these two figures are very similar to those seen in the radon dataset. The greatest anomalies tend to be observed closest to the event epicenters, and the start times and the times of the greatest anomalies tend to increase with the magnitude of the coming earthquake. Also, there is a hint in Fig. 7 that the greatest groundwater level changes may be associated with the largest magnitude events. As for the gas emission data, the significant amount of scatter in the groundwater data precludes the determination of any useful regression curves as a function of either distance or magnitude. Here also curves that represent the possible extremal values from the data are plotted in Figs. 7 and 8, and the corresponding equations for these lines are summarized in Table 4.

In many ways, many of the characteristics of the groundwater change precursors documented in this study, such as the time of the initiation of the anomalies, the time of the greatest anomaly, and the dependence of the amplitude of the anomaly on magnitude and epicentral distance, seem to parallel the same characteristics in the radon gas anomalies. This is probably because both phenomena are associated with changes in rock permeability and perhaps porosity during the days, weeks and perhaps months before an earthquake rupture initiates.

4.13. Groundwater level change models

Changes in groundwater levels have been observed before certain earthquakes and are believed to be in response to volumetric strain in the earth's crust. However, in order to determine the groundwater level changes are directly related to crustal strain, nontectonic causes of water level changes must be considered. These include barometric pressure changes, tidal effects, rainfall, and extraction of groundwater and other fluids such as oil and gas. A summary of evaluating groundwater level changes as earthquake precursors is given by Roeloffs (1988).

The largest precursory water level changes are observed in confined aquifers (Roeloffs and Quilty, 1997). For these aquifers, the change in reservoir fluid pressure Δp is related to the incremental change in volumetric strain Δe by (Rice and Cleary, 1976)

$$\Delta p = -(2GB/3)[(1+\nu_u)/(1-2\nu_u)]\Delta e, \tag{12}$$

where G is the shear modulus, B is Skempton's coefficient, and n_u is the undrained Poisson's ratio. The change in water level Δh is related to Δp by

$$\Delta h = \frac{\Delta p}{\rho g}, \tag{13}$$

where r is the fluid density and g is the gravitational acceleration. For typical values of $G = 3$ Gpa, $B = 0.8$, and $n_u = 0.3$, the water level change would be 52 cm per 10^{-6} strain (Roeloffs, 1988), with a rise in water level corresponding to compressive strain and a drop in water level corresponding to dilatational strain.

For unconfined aquifers, the water level change is given by

$$\Delta h = -(H/n)\Delta e, \tag{14}$$

where H is the saturation thickness of the aquifer and n is the porosity. For a 100 m saturated aquifer with 2% porosity, the expected change in water level is 0.5 cm per 10^{-6} strain (Roeloffs, 1988), significantly less than that for a confined aquifer.

As mentioned above, water level changes due to nontectonic origin can occur and must be accounted for in order to accurately determine the amount of water level change due to crustal strain. Barometric pressure changes can contribute to changes in water levels in a groundwater aquifer. An increase in barometric pressure Δb compresses the aquifer, causing the pressure in the aquifer to increase by

$$\Delta p = (b/3)[(1+\nu_u)/(1-\nu_u)]\Delta b. \tag{15}$$

In an open well, however, the increase in barometric pressure causes a downward force on the fluid surface, counteracting the effect

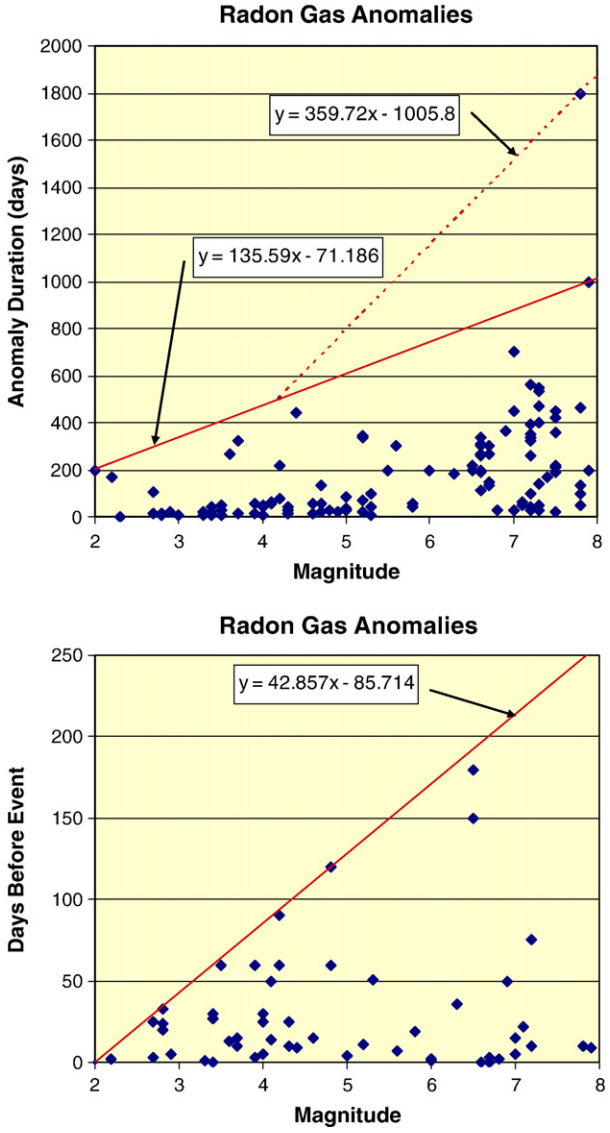

Fig. 4. Distribution of the initiation times (top) and durations (bottom) of the radon anomalies with event magnitude. The greatest initiation times and anomaly durations are associated with the largest earthquakes. Curves representing the possible extremal values of the data sets are also shown. On the top figure, the solid extremal line ignores the one extreme data point at about magnitude 8, while the combination of the solid and dashed extremal lines include this data point.

of the increase in the reservoir fluid pressure. The net effect is a decrease in water level given by

$$\Delta h = -(1/\rho g)[1 - (B/3)(1+\nu_u)(1-\nu_u)]\Delta b. \quad (16)$$

This relation predicts a decrease of 0.52 cm in water level per 1 mbar of pressure change (Roeloffs, 1988).

Another important effect that causes changes in water levels is the earth's tidal response. The change in water level due to the earth's tidal response is given by

$$\Delta h = -\frac{K\Delta e}{n\rho g}, \quad (17)$$

where Δe is now the volumetric strain induced in the earth by the tidal response and K is the bulk modulus of water (Bredehoeft, 1967). This relation assumes the compressibility of the individual rock grains is negligible compared to the compressibility of the reservoir, and it is not valid for low porosities. This relation can be used with a porosity vs. depth relation to determine the sensitivity to the tidal response as a function of depth.

Roeloffs (1988) discusses the effect of rainfall on groundwater level changes. Rainfall acts to recharge the aquifer by providing a transient source of fluid into the reservoir. Similar effects can also be considered when fluids are withdrawn from aquifers.

The effects of rainfall are often delayed by some period of time, depending on the thickness and permeability of the overburden, and the distance between the rainfall source. This time delay can be as long as several months. In addition, a threshold amount of rainfall may be required before reservoir recharge is initiated.

4.14. Ground temperature change observations

There have been relatively few reported observations of temperature changes in the earth prior to earthquakes. This is probably due to a lack of experiments to look for such an effect. The thermal

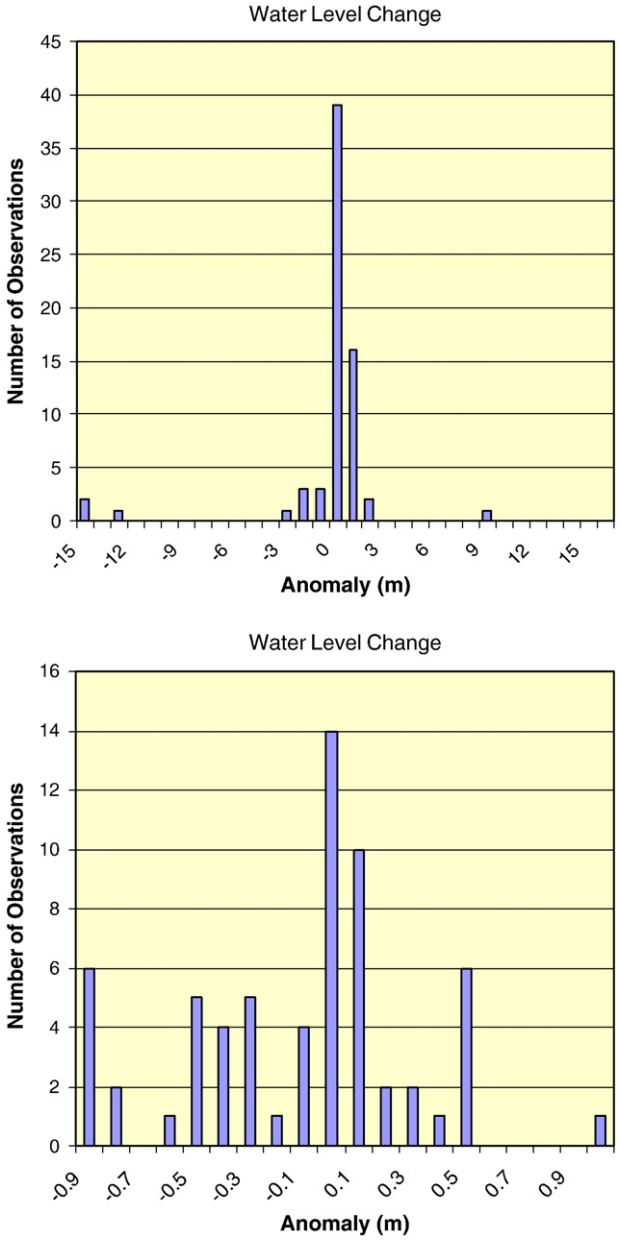

Fig. 5. Distribution of reported maximum changes in groundwater level prior to earthquakes. The top plot shows all the observations, while the bottom plot shows the observations of water level changes between −1 m and +1 m.

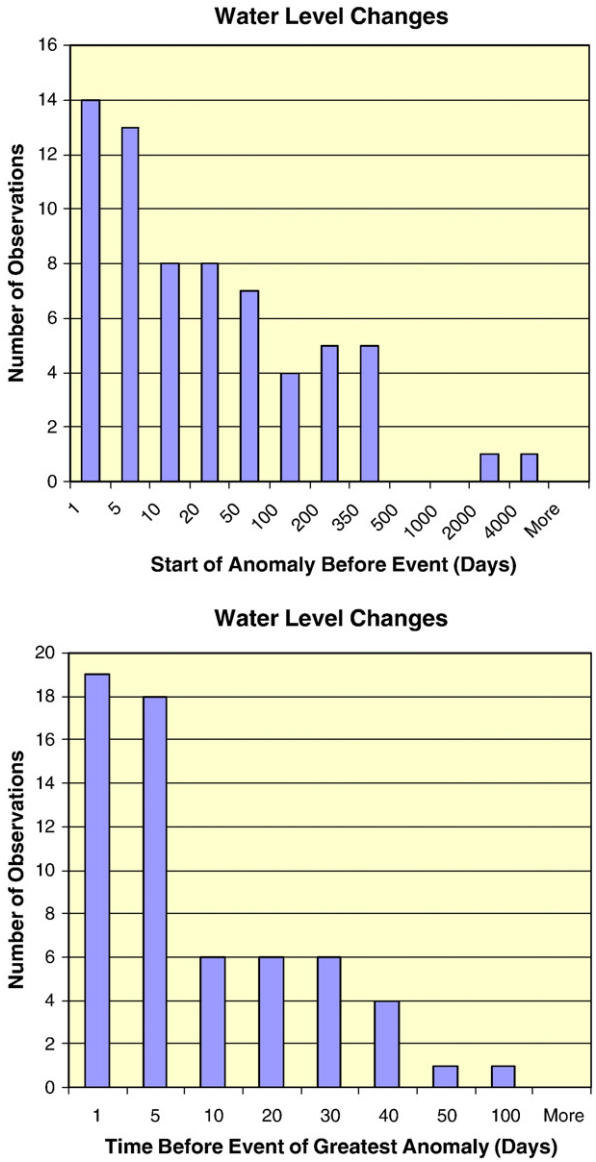

Fig. 6. Distribution of reported times of initiation of the groundwater anomaly prior to the earthquake (top) and of the times of the greatest groundwater change (bottom).

conductivity of rock is quite low, and it takes many years for a significant temperature change to diffuse just a few meters in rocks. Thus, from a theoretical point of view, one would not expect to observe thermal anomalies in rocks prior to earthquakes.

On the other hand, as documented above the flow of groundwater and gases through the rocks and soils might be altered during some time period before an earthquake occurs in a region. Particularly in areas of active tectonics and volcanics, such alterations of the flow of water in the earth before an earthquake might sometimes allow that water to come into contact with hotter rock bodies at depth and raise the temperatures of near-surface groundwaters. In some cases, the alterations in the rock pore structure at depth before an earthquake might cut off a flow of geothermally warmed water to the surface, leading to a cooling of near-surface water temperatures. Of these two possible scenarios for precursory temperature changes, the former would be easier to observe since the rock and soil around the cooler water would remain at a warmer temperature for a long period of time due to the poor thermal conductivity of the rock and soil.

The temperature change dataset assembled in this study consisted of 15 observations from 12 earthquakes ranging in magnitude from 2.3 to 7.0 (Table 5). Of the 15 observations, 10 reports came from measurements taken at hot springs in volcanic areas. Most of the observations were taken within 50 km of the epicenters of the coming earthquakes, although the greatest reported epicentral distance for an anomaly was 470 km. In all cases an increase in ground temperature was reported, with the largest change being 6 °C and most of the changes being <1 °C. Five of the temperature changes in groundwater were reported to have been coseismic, i.e., having occurred at the time of the earthquake, while 5 were reported to take place within the 10 days prior to the earthquake. The rest of the observations did not report the time at which the temperature change was reported.

All of these reported changes in temperature associated with earthquakes were from Greece and Japan. Both are areas of active plate subduction with active volcanoes and numerous geothermal features. It is not known if there might be temperature changes in the groundwater of non-geothermal areas prior to earthquakes, as there

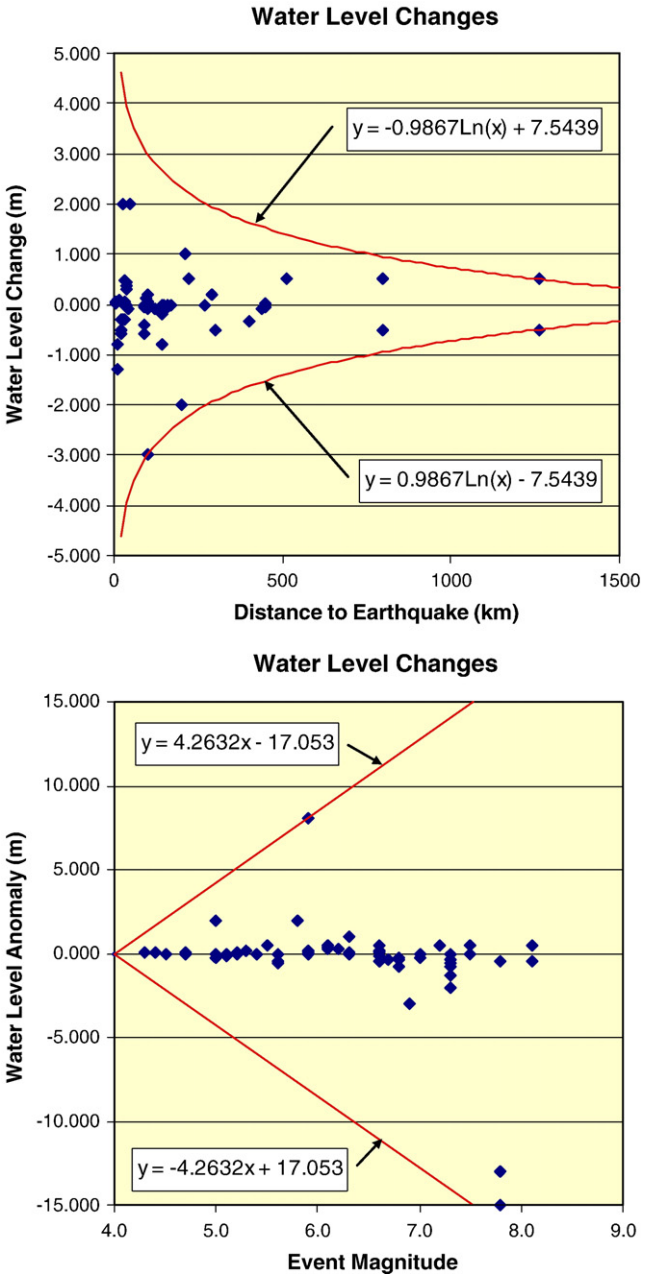

Fig. 7. Distribution of reported changes in maximum groundwater level with distance to the earthquake (top) with event magnitude (bottom). The greatest anomalies are reported closest to the epicenters and perhaps for the largest earthquakes. Curves representing the possible extremal values of the data sets are also shown.

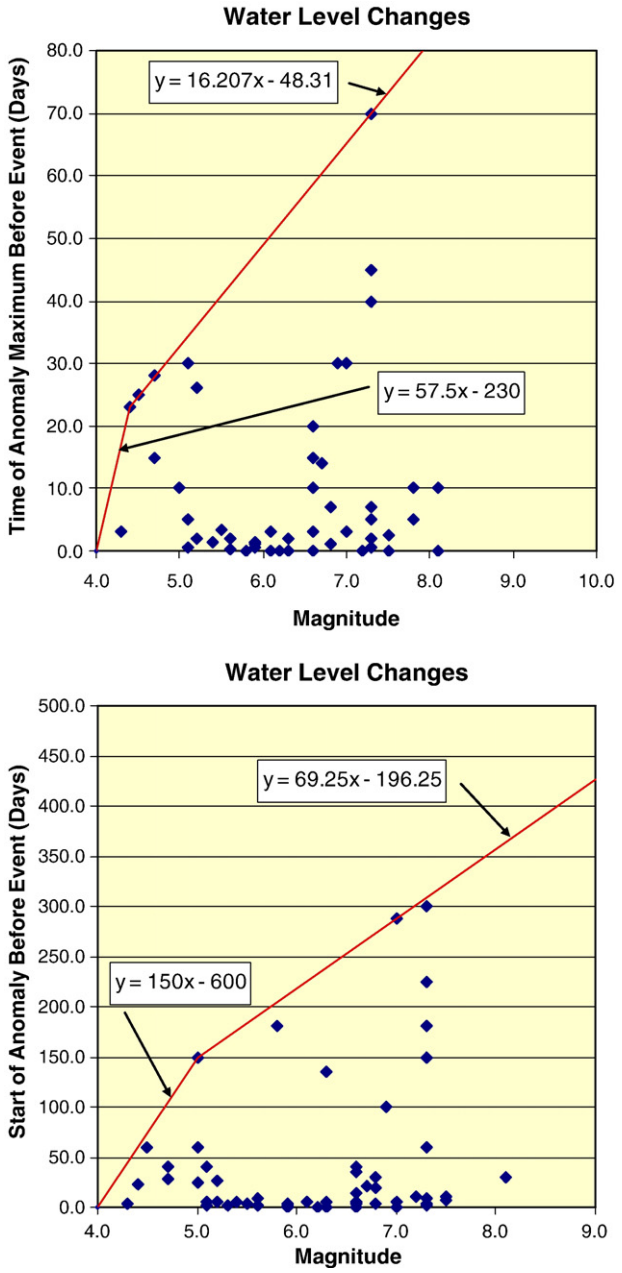

Fig. 8. Distribution of the times of the greatest groundwater changes (top) and of the start time of the groundwater changes (bottom) with event magnitude. The greatest groundwater level changes and start times are associated with the largest earthquakes. Piecewise linear curves representing the possible extremal values of the data sets are also shown.

have been no reported studies. However, it is possible that such would not be the case. The San Andreas Fault has no geothermal anomaly associated with it (e.g., Lachenbruch and Sass, 1992), an unexpected observation because shear strain heating from the multitude major earthquakes on that fault over geologic time was thought to have led to an increase in heat flow and rock temperatures in the vicinity of that fault. This observation could mean that temperature changes may not take place prior to earthquakes in non-volcanic or geothermal areas.

4.15. Ground temperature change models

Precursory temperature anomalies are usually associated with changes in groundwater levels and with geochemical anomalies, although frictional heating on fault surfaces could contribute to ground temperature changes. Because rocks have a relatively low thermal conductivity, any such temperature-related changes that may occur at depth in the earth would take a long time to reach the surface. Therefore such a temperature anomaly is expected to be relatively small.

Temperature anomalies associated with groundwater level changes could be significant, however. Heat generated at depth within the earth would be more efficiently transported to the surface by the convective flow of groundwater than by thermal conduction through the rock itself. Should pre-earthquake dilatancy be a significant pre-earthquake effect, the opening of new pores and the widening of old pore as the rock becomes dilatant may allow groundwater and gases trapped in the rock to circulate through deeper, and therefore warmer, rock. Near the surface of the earth, geothermal gradients can be 1.5 °C–3.5 °C per 100 m, except at geothermal areas and volcanoes where they can be much higher. Thus, if the groundwater is suddenly allowed to circulate through rock that is 200 m deeper than before the dilatancy began, then the surface groundwater may increase in temperature by several degrees. The amount of temperature increase that would observed at the surface would be controlled by the depth to which the groundwater would circulate, the temperatures at the new depths where the water is circulating, the speed at which the deep groundwater would come to the surface, and the ratio of the volumes of the deep and shallow groundwaters.

4.16. Surface deformation observations

There has been a longstanding interest in looking for surface deformations (uplifts, downdrops, tilts, strains, strain rate changes, etc.) prior to earthquakes (Rikitake, 1976). Many crustal earthquakes of M6 and greater have been associated with deformations at the surface of the earth, and in some cases there is evidence that there were deformations that were precursory to the occurrences of the earthquakes (Rikitake, 1976; Lomnitz, 1994). Unfortunately, until very recently, documenting such changes has been very difficult. Surface leveling and laser-ranging geodetic measurements were the most accurate way to document ground deformations over regions that are tens of kilometers in dimension. However, such measurements are time consuming and expensive to make, and the feasible time between individual measurements is months to years. Modern GPS and satellite-based SAR interferometry measurements are now available to produce geodetic position changes with individual measurements separated by minutes to days. However, these new technologies have yet to capture surface deformations precursory to strong earthquakes.

The sparse ground-deformation dataset compiled in this study (Table 6) reflects the formerly difficult nature of making such measurements prior to earthquakes and the lack of successful precursory measurements using the new technologies. We compiled a dataset of 12 tilt observations from 9 earthquakes, 5 strain observations from 2 earthquakes, and 3 strain rate change observations from 1 earthquake. The earthquakes ranged in magnitude from 3.0 to 7.1. Most of the measurements were made at epicentral distances of less than 100 km, although the measurements range as far as 400 km from the epicenter in one case. The reported deformations took place months to days before the earthquakes, and the larger amplitude strains and tilts seem to be associated with the larger earthquakes.

4.17. Surface deformation models

Models to predict surface deformation in the vicinity of a fault involve the ability to model the behavior of the fault itself. These models can indicate what type of surface deformations can occur and

Table 5
Reported precursory temperature changes associated with earthquakes.

Earthquakes with reported temperature–variation precursors								
Earthquake	Mag.	Date	Precursor time	Anomaly [°c][a]	Ambient temp before eq [°c]	Dist. from epicenter [km]	Ref.	Notes
Thessaloniki, Greece	4.8	10/20/1998	2 days	0.2	16.6	33	Asteriadis and Livieratos, 1989	From well data
Thessaloniki, Greece	4.8	10/20/1998	5 days	0.7	15.5	41	Asteriadis and Livieratos, 1989	From well data
Thessaloniki, Greece	4.8	10/20/1998	Coseismic	0.7	17.6	41	Asteriadis and Livieratos, 1989	From well data
Thessaloniki, Greece	4.8	10/20/1998	Coseismic	0.5	19.8	41	Asteriadis and Livieratos, 1989	From well data
Bay of Patras, Greece	5.4	7/14/1993	12 h	6	17	1.5	Soter, 1999	From sea bed (20 m below surface, 10 m above sea bed, 650 m from shore)
Kawazu, Japan	5.4	1976	Not reported[b]	0.3	60	28	Mogi et al., 1989	From hot springs data
Izu–Oshima–Kinkai, Japan	7	1978	10 days	1.3	59.5	31	Mogi et al., 1989	From hot springs data
Miyagi–Ken–Oki, Japan	7.4	1978	Not reported[b]	0.6	60	470	Mogi et al., 1989	From hot springs data
Ito–Oki, Japan	5.4	1978	Not reported[b]	1.2	59.8	16	Mogi et al., 1989	From hot springs data
Ito–Oki (swarm), Japan	3.8	1979	Not reported[b]	0.5	59.3	10	Mogi et al., 1989	From hot springs data
Izu–Hanto–Toho–Oki, Japan	6.7	1980	3 days	1.75	59	16	Mogi et al., 1989	From hot springs data
Ito–Oki, Japan	3.7	1981	Not reported[b]	0.5	59.5	11	Mogi et al., 1989	From hot springs data
Sagami Bay, Japan	5.7	Aug-82	Coseismic	1	59.7	46	Mogi et al., 1989	From hot springs data
Ito–Oki, Japan	2.3	Jul-82	Coseismic	0.7	59.4	6	Mogi et al., 1989	From hot springs data
Ibaraki–Ken–Oki, Japan	7	Jul-82	Coseismic	0.6	59	290	Mogi et al., 1989	From hot springs data
Datong, China	6.1	10/18/1989	2 days	2–4 avg., 5–6 max.	10	£ 200	Qiang et al., 1997	Thermal infrared satellite (Meteosat)
Oroville, California	5.8	8/1/1975	1 day	>100 min	50 min	<200	Valette-Silver and Silver, 1991; Silver and Valette-Silver, 1992	Old Faithful Geyser, Calistoga, California (eruption interval data)
Morgan Hill, California	6.1	4/24/1984	1 day	25 and 50 min (bimodal signal)	40 min	<200	Valette-Silver and Silver, 1991; Silver and Valette-Silver, 1992	Old Faithful Geyser, Calistoga, California (eruption interval data)
Loma Prieta, California	7.1	10/18/1989	60 h	172 min	90 ± 2 min	180	Silver et al., 1990; Valette-Silver and Silver, 1991; Silver and Valette-Silver, 1992	Old Faithful Geyser, Calistoga, California (eruption interval data)

[a] Positive, unless otherwise indicated.
[b] It is inferred from the paper that these precursors are on the order of a couple months, but it is not clearly stated.

whether or not these deformations are likely to be detected with the available surface instruments.

Fault models attempt to specify the mechanical behavior along the faults. This mechanical behavior is modeled using a constitutive relationship that defines the rate- and state-dependent behavior of friction along the fault surface. Dieterich (1972; 1978; 1979) defined such a law and Ruina (1983) later modified it. The steady-state coefficient of friction μ_{ss} is given by

$$\mu_{ss}(V) = \mu^* + (\mathbf{a} - \mathbf{b}) \ln(V / V^*), \tag{18}$$

where V is the slip velocity, V^* is an arbitrary reference velocity such that $\mu_{ss}(V^*) = \mu^*$, and **a** and **b** are constitutive parameters. The parameter **a** is a measure of the magnitude of the instantaneous change in the coefficient of friction as the velocity changes, and **b** is a measure of the decay in the coefficient of friction at the new velocity. The decay of the coefficient of friction is exponential with decay constant D_c, called the characteristic decay distance.

An alternative form of the constitutive relation for the fault is given by Tse and Rice (1986). This form uses shear stress instead of the coefficient of friction and is given by

$$\tau_{ss}(V) = \tau^* + \sigma_n(\mathbf{a} - \mathbf{b}) \ln(V / V^*), \tag{19}$$

where t_{ss} is the steady-state shear stress, s_n is the normal stress, and $t^* = t_{ss}(V^*)$.

Lorenzetti and Tullis (1989) used the Tse and Rice (1986) model to study crustal strike-slip earthquakes and to calculate displacement, velocity, strain, and strain rate distributions associated with these earthquakes. Their results indicate that strain rates are the most readily detectable signals, because the magnitudes of these signals are larger than the detectability thresholds of strains by current instrumentation due to the presence of noise that cannot yet be removed from the data.

4.18. Precursory seismicity observations

This precursor is well studied by ground-based seismic instruments, but it is included here for two reasons. First, because many of the earth's strong earthquakes are preceded within hours, days or weeks by smaller earthquakes called foreshocks, this premonitory seismic activity may well be related in some way to the non-seismic precursors described above. Second, in principle, satellite-based detection of seismic ground motions is possible, and in the future there may be interest in developing such a technology to complement surface-based observations.

No formal table of foreshock observations was compiled for this study, as the list would be very extensive but not particularly informative for the purposes of this paper. However, we present here some summary statistics of earthquake foreshock activity from published analyses.

The most important summaries of foreshocks on a global basis were published by Jones and Molnar (1976) and Reasenberg (1999). The former study reported on $M>7.0$ earthquakes from 1950 to 1973 and showed that 44% of these strong earthquakes had a least one foreshock ($M>4.5$) within 40 days of the main shock. The latter study analyzed $M>6.0$ earthquakes from 1977 to 1996 and showed that 13.2% had a least one foreshock ($M>5.0$) with 10 days and 75 km of the main shock. It is likely that many earthquakes have smaller foreshocks than those reported in these studies, and so these results probably represent a lower bound on global foreshock rates before strong earthquakes. However, no statistical work to document the rates of smaller magnitude foreshocks has been done due to uneven earthquake detection worldwide.

One significant point of these foreshock studies is that most foreshocks seem to take place during the same time period (within

Table 6
Reported measured precursory ground deformations associated with earthquakes.

Earthquakes with reported ground-deformation precursors								
Area	Date	*M*	Type	*D* [km]	Anomaly	Time before event	References	Notes
San Andreas Fault, California	7/73 to 3/7 (28 events)	2.5–4.3	Tilt	<30 km	2×10^{-6} (tilt direction often changes prior to earthquakes)	Typicallty 1 month	Johnston and Mortensen, 1974	
Kalapana, Hawaii	11/29/1975	7.2	Strain		3.5×10^{-4}	5 months	Wyss et al., 1981	
Friuli, Italy	5/6/1976	6.5	Tilt	15	200 sec	3 years	Dragoni et al., 1985	
Friuli, Italy	9/15/1976	6.5	Tilt	15	200 sec	3 years	Dragoni et al., 1985	
Izu–Oshima, Japan	1/14/1978	7.0	Compressional strain change S of epicenter		2.5×10^{-6}	6 weeks	Linde and Suyehiro, 1983	
Izu–Oshima, Japan	1/14/1978	7.0	Compressional strain change NE of epicenter		4×10^{-5}	days	Linde and Suyehiro, 1983	
Homestead Valley, California	1/21/1979	3.1	Pre-seismic creep	32	−100 mm	40 h	Leary and Malin, 1984	
Homestead Valley, California	2/17/1979	2.0	Pre-seismic creep	8	+100 mm	5 days	Leary and Malin, 1984	
Homestead Valley, California	3/9/1979	2.4	Pre-seismic creep	24	−200 mm	2 days	Leary and Malin, 1984	
Homestead Valley, California	3/15/1979	5.1	Pre-seismic creep	150	−100 mm	20 h	Leary and Malin, 1984	
Lytle Creek, California	10/19/1979	4.1	Stress transient	15	0.14 MPa	2–4 weeks	Clark, 1981	
Irpinia, Italy	11/23/1980	6.5	Tilt	250	1.5×10^{-5} radians	2 months	Allegri et al., 1983	
Irpinia, Italy	11/23/1980	6.5	Tilt	250	2×10^{-5} radians	6 months	Allegri et al., 1983	
Kamchatka Gulf	8/17/1983	6.9	Leveling	100	2.4 mm/day	2 days	Fedotov et al., 1992	
Friuli region, Italy	2/1/1988	4.1	Tilt	1.8	1.5×10^{-5} radians	2 months	Dal Moro and Zadro, 1999	
Friuli region, Italy	10/5/1991	3.9	Strain	2.9	9×10^{-7}	9 days	Dal Moro and Zadro, 1999	
Spitak, Armenia	12/7/1988	6.9	Strain	100	3×10^{-7}	0–8 days	Neresov and Latynina, 1992	1, 2
Spitak, Armenia	12/7/1988	6.9	Tilt	100	1×10^{-7}	0–8 days	Neresov and Latynina, 1992	1, 2
Spitak, Armenia	12/7/1988	6.9	Strain	125	1×10^{-8}	0–8 days	Neresov and Latynina, 1992	1, 2
Spitak, Armenia	12/7/1988	6.9	Strain	300	1.5×10^{-6}	0–8 days	Neresov and Latynina, 1992	1, 2
Spitak, Armenia	12/7/1988	6.9	Tilt	300	2×10^{-5}	0–8 days	Neresov and Latynina, 1992	1, 2
Spitak, Armenia	12/7/1988	6.9	Strain	400	9×10^{-7}	0–8 days	Neresov and Latynina, 1992	1, 2
Spitak, Armenia	12/7/1988	6.9	Tilt	400	1×10^{-7}	0–8 days	Neresov and Latynina, 1992	1, 2
Loma Prieta, California	10/17/1989	7.1	Strain rate change	31	From −10.8 1.0 to −18.9±5.0 mm/yr	1.3 years	Lisowski et al., 1990	
Loma Prieta, California	10/17/1989	7.1	Strain rate change	31	From 6.6±1.1 to 2.0±5.0 mm/yr	1.3 years	Lisowski et al., 1990	
Loma Prieta, California	10/17/1989	7.1	Strain rate change	43	From −8.7±1.5 to −23.8±7.1 mm/yr	1.3 years	Lisowski et al., 1990	
Loma Prieta, California	10/17/1989	7.1	Creep retardation	0–80 (6 sites)	From 10.3 to 6.8 mm/yr	July 1987 to September 1989	Breckenridge and Burford, 1990	
Central Appenines, Italy	4/3/1991	3.3	Tilt	7.6	1.34×10^{-7}	months	Bella et al., 1995a,b	3
Central Appenines, Italy	7/13/1991	3.7	Tilt	35.8	6×10^{-9}	months	Bella et al., 1995a,b	3
Central Appenines, Italy	5/5/1992	3	Tilt	11.5	1.4×10^{-8}	months	Bella et al., 1995a,b	3
Central Appenines, Italy	8/25/1992	3.9	Tilt	23.1	3.8×10^{-8}	months	Bella et al., 1995a,b	3
Central Appenines, Italy	8/27/1992	3.1	Tilt	9.1	3.9×10^{-8}	months	Bella et al., 1995a,b	3
Central Appenines, Italy	10/24/1992	3.7	Tilt	27.7	1.1×10^{-8}	months	Bella et al., 1995a,b	3
Central Appenines, Italy	10/24/1992	3.5	Tilt	27.7	6×10^{-9}	months	Bella et al., 1995a,b	3
Central Appenines, Italy	7/16/1993	3.5	Tilt	28	6×10^{-9}	months	Bella et al., 1995a,b	3
Hollister, Calfiornia	11/28/1974	5.2	Tilt	11.2	7×10^{-6} radians	30 days	Mortensen and Johnston, 1976	
Briones Hills, California	1/8/1977	4.3	Tilt	5.5	2×10^{-6} radians	1 month	Jones et al., 1977	
Calaveras Fault, California	8/29/1978	4.2	Tilt	6.0	8.6×10^{-6} radians	63 h	Iwatsubo and Mortensen, 1979	
Calaveras Fault, California	8/29/1978	3.9	Tilt	4.5	8.6×10^{-6} radians	63 h	Iwatsubo and Mortensen, 1979	
Calaveras Fault, California	9/5/1978	2.5	Tilt				Iwatsubo and Mortensen, 1979	
Niigata, Japan	6/16/1964	7.5	Vertical crustal movement	30	5 cm	5 years (1959–1964)	Fujii and Nakane, 1997	
Japan Sea	5/26/1983	7.7	Strain (about 100 events)	90	1×10^{-8} to 3 10^{-8} (typically 3 h duration)	5 months	Linde et al., 1988	
Joshua Tree, California	4/23/1992	6.1	Fault normal extension		30±3 mm	3/8/1992–3/9/1992	Shifflett and Witbaard, 1996	
Landers, California	6/28/1992	7.3	Fault normal extension		30±3 mm 24±6 mm	6/7/1992–6/8/1992 6/6/1992	Shifflett and Witbaard, 1996	
Landers, California	6/28/1992	7.3	Horizontal slip (dextral)		20±9 mm 24±6 mm	6/6/1992	Shifflett and Witbaard, 1996	
Big Bear, California	6/28/1992	6.2	Fault normal extension		30±3 mm 24±6 mm	6/7/1992–6/8/1992 6/6/1992	Shifflett and Witbaard, 1996	
Big Bear, California	6/28/1992	6.2	Horizontal slip (dextral)		20±9 mm 24±6 mm	6/6/1992	Shifflett and Witbaard, 1996	
Tonankai, Japan	12/7/1944	8.1	Uplift		4 mm	1 day	Mogi, 1985	
Tonankai, Japan	12/7/1944	8.1	Tilt		1×10^{-5} sec	1 day	Mogi, 1985	

[1]These values are approximate, as they were read off a figure.
[2]The background signal (i.e., tidal strain) levels are not available from this report.
[3]The exact precursor times are not provided.

about 30 days of the main shock) when the most frequently reported non-seismic precursors (i.e., radon anomalies, groundwater level changes, EM emissions) seem to take place. Thus, it is possible that there are some physical links in the generation mechanisms of all of these precursors.

4.19. Precursory seismicity models

Scholz (1990) argued that foreshock activity is probably a manifestation of the nucleation process that ultimately results in the main earthquake. He noted that foreshocks tend to occur in the immediate vicinity of the hypocenter of the later main shock, they increase in frequency of occurrence as the time of the main shock is approached, and they are typically much smaller in magnitude than the main shock. Dilatancy may explain short-term quiescences just prior to the main shock in some foreshock sequences. The models for precursory crustal deformation, described earlier, also can be applied to explain foreshock sequences since rapid crustal deformations may be associated with some seismic energy release. The individuality of foreshock sequences from one earthquake to another may mean that foreshocks are not an intrinsic part of the nucleation process on a fault but rather are part of that nuclear process (Scholz, 1990).

5. Discussion of the observations and models of earthquake precursors

The data and analyses described in the previous sections can be combined to make some general statements about the characteristics of anomalous precursors that may precede earthquakes. From the observational data, it appears that the largest amplitude anomalies tend to occur before the largest magnitude earthquakes. This seems most clear for the groundwater level and the gas emission datasets, while there are insufficient data to generalize this argument for the other precursors looked at in this study. Nevertheless, such a characteristic is implicit in the physical models describing all of the precursors. A second common characteristic for all of the precursors is that the strongest anomalies seem to occur within about 1 month of the coming earthquake, and the closer in time to the occurrence of the earthquake, the larger the number of precursor types that might be observed. The observations of increasing EM anomalies and foreshock activity in the hours just prior to many earthquakes suggest that this might be a critical preparatory time in a fault region just before an earthquake occurs.

For all of the precursor types researched here, it appears that most of the anomalies tend to be observed within a couple hundred kilometers of the coming earthquake epicenter. This is consistent with the scaling relationships of fault length and earthquake magnitude. Large earthquakes move large volumes of rock in the earth. For example, the average fault lengths for earthquakes of magnitude 5, 6, 7 and 8 are approximately 5 km, 15 km, 40 km, and 100 km, respectively. Thus, most precursory earthquake anomalies seem to be observed in or near the region in the earth where the largest deformations are experienced in the eventual earthquake. There are some important implications of the size of the area around an earthquake epicenter where precursory phenomena might be observed. First, if an anomaly suggesting a coming earthquake is observed, the area on the earth in which that earthquake might take place is relatively limited, giving some spatial resolution for earthquake predictions. Second, it is currently not known how large a surface area on the earth may emit an EM anomaly, show a radon anomaly, or experience a groundwater change prior to an earthquake.

The models for the various earthquake precursors analyzed in this study also have some important common features. The most important common feature is that the earthquake precursory anomalies are thought to be driven by rapid and probably non-linear strain and strain changes within the earth in the rock near or in the fault zone at the region of the eventual earthquake rupture. Non-linear stress–strain and dilatant behavior prior to rock fracture has long been observed in laboratory experiments when small pieces or rock (a few cm on a side) are fractured (Scholz, 1990). The rapid deformations just prior to fracture combined with changes in the groundwater and gas flow in the earth due changes in porosity and permeability in the rock volume that fractures in the earthquake can generate, in one way or another, all of the earthquake precursors studied here (e.g., Press and Siever, 1978; Lomnitz, 1994). It is not known how well the small-scale laboratory experiments may apply to the large-scale rupture processes that take place within the earth. Also, there are many free parameters that are poorly known in the models discussed in the previous section of this report. Nevertheless, the laboratory experiments and theoretical models do provide some plausible physical explanations for the observed earthquake precursory data.

Regarding individual precursors, some comments should be made about the observational data. The EM observations compiled in this study give a somewhat confused picture about exactly what kinds of precursory signals might be seen before earthquakes. The frequency content of the observed anomalous signals compiled in our work seems to vary considerably from study to study. One study indicates that the anomalous precursory signals are confined in latitude but observed at a wide range of longitudes, while another study show confinement of the anomalous signals over a narrow longitude band but at essentially all latitudes. Much still probably must be learned about precursory EM signals and earthquakes. We point out that there was one surface-based observation of a strong ionospheric signal at about 4–5 MHz recorded at Boulder, Colorado that started about 2 h before the great Alaskan earthquake of 1964 (Davies and Baker, 1965). This earthquake (M9.2) was the second largest earthquake known since earthquake recording began in the late 1800s. Thus, as with the 1989 Loma Prieta ULF observation, there are some provocative observations that suggest that the earth may well radiate EM energy at perhaps many different frequencies prior to the initiation of a strong earthquake.

The paucity of studies of temperature change data prior to earthquakes is most consistent with the lack of interest in this topic by most earthquake scientists. There have been very few experiments to look for such a phenomenon. Furthermore, the lack of a heat flow anomaly at the San Andreas Fault may mean that San Andreas earthquakes are not accompanied by precursory temperature changes. Even so, in volcanic areas that are also prone to strong earthquakes, changes in the flow of groundwater and gas emission may be accompanied by anomalous changes in the temperature of the surface groundwater and gas emissions. This could be a target for future space-based research. It could also have application in the search for the imminence of major volcanic eruptions.

Surface deformations precursory to earthquakes are of interest to seismologists. In part this is because laboratory and theoretical rock deformation studies prior to fracture, especially the observation of dilatancy in rocks just prior to their fracture, indicate that in many cases surface deformations might be observed. As noted above it has been very expensive, laborious and time consuming to make surface deformation observations in the past. The advent of relatively inexpensive continuous GPS observations and of methods to measure ground deformations using satellite-based synthetic aperture radar interferometry (IN-SAR) are rapidly changing the way that surface deformations will be observed for scientific studies. For example, the Plate Boundary Observatory (PBO) is a major effort by the NSF to fund a very large number of continuous, permanent GPS stations in the western U.S. The purpose of the PBO is to monitor real-time deformation of the western plate boundary of North America (Silver, 1998). Thus, in the future many of the past constraints limiting surface deformation studies in earthquake-prone areas are likely to be eliminated.

Acknowledgements

The authors would like to thank the Center for Subsurface Sensing and Imaging Systems (CenSSIS) at Northeastern University. This research was supported by the National Reconaissance Office (NRO) under Contract No. C-0097.

References

Alimova, V.A., Zubkov, S.I., 1983. Catalog of earthquake precursors. Hydrogeodynamic Precursors: Institute of Physics of the EarthAkad. Nauk SSSR, Moscow. (140 pp. in Russian).

Allegri, L., Bella, F., Della Monica, G., Ermini, A., Improta, S., Sgrigna, V., Biagi, P.F., 1983. Radon and tilt anomalies detected before the Irpinia (south Italy) earthquake of November 23, 1980 at great distances from the epicenter. Geophys. Res. Lett. 10, 269–272.

Asteriadis, G., Livieratos, E., 1989. Pre-seismic responses of underground water level and temperature concerning a 4.8 magnitude earthquake in Greece on October 20, 1998. Tectonophysics 170, 165–169.

Bakun, W.H., Lindh, A.G., 1985. The Parkfield, CA earthquake prediction experiment. Science 229, 619–624.

Barsukov, V.L., Varshal, G.M., Zamokina, N.S., 1985. Recent results of hydrogeochemical studies for earthquake prediction in the USSR. Pure Appl. Geophys. 122, 143–156.

Bella, F., Biagi, P.F., Caputo, M., Cozzi, E., Della Monica, G., Ermini, A., Plastino, W., Sgrigna, V., Zilpimiani, D., 1995a. Helium content in thermal waters in the Caucasus from 1985 to 1991 and correlations with the seismic activity. Tectonophysics 246, 263–278.

Bella, F., Biagi, P.F., Caputo, M., Della Monica, G., Ermini, A., Manjgaladze, P.V., Sgrigna, V., Zilpimiani, D.O., 1995b. Possible creep-related tilt precursors obtained in the central Apennines (Italy) and in the southern Caucasus (Georgia). Pure Appl. Geophys. 144, 277–300.

Bella, F., Biagi, P.F., Caputo, M., Cozzi, E., Della Monica, G., Ermini, A., Plastino, W., Sgrigna, V., 1998. Field strength variations of LF radio waves prior to earthquakes in central Italy. Phys. Earth Planet. Inter. 105, 279–286.

Bernard, P., Pinettes, P., Hatzidimitriou, P.M., Scordilis, E.M., Veis, G., Milas, P., 1997. From precursors to prediction: a few recent examples from Greece. Geophys. J. Int. 131, 467–477.

Biagi, P.F., Ermini, A., Cozzi, E., Khatkevich, Y.M., Gordeev, E.I., 2000a. Hydrogeochemical precursors in Kamchatka (Russia) related to the strongest earthquakes in 1988–1997. Nat. Hazards 21, 263–276.

Biagi, P.F., Ermini, A., Kingsley, S.P., Khatkevich, Y.M., Gordeev, E.I., 2000b. Groundwater ion content precursors of strong earthquakes in Kamchatka (Russia). Pure Appl. Geophys. 157, 1359–1377.

Biagi, P.F., Ermini, A., Kingsley, S.P., 2001. Disturbances in LF radio signals and the Umbria–Marche (Italy) seismic sequence in 1997–1998. Phys. Chem. Earth (C) 26, 755–759.

Borchiellini, S., Bernat, M., Campredon, R., 1991. Ground variation of radon 222 for location of hidden structural features: example of the south of France (Alpes Maritimes). Pure Appl. Geophys. 135, 625–638.

Breckenridge, K.S., Burford, R.O., 1990. Changes in fault slip near San Juan Bautista, California before the October 17, 1989 Loma Prieta earthquake — a possible precursor? Eos, Trans.-Am. Geophys. Union 71, 1461.

Bredehoeft, J.D., 1967. Response of well-aquifer systems to earth tides. J. Geophys. Res. 72, 3075–3087.

Byerlee, J., 1993. Model for episodic flow of high-pressure water in fault zones before earthquakes. Geology 21, 303–306.

Cai, Z.H., Shi, H.X., 1980. An Introduction to Seismological Fluid Geology. Seismological Press, Beijing. (268 pp. in Chinese).

Chadha, R.K., Pandey, A.P., and Kuempel, H.J., (2003). Search for earthquake precursors in well water levels in a localized seismically active area of reservoir triggered earthquakes in India, Geophys. Res. Lett., 30, 1416 Geophys. Res. Lett., 31, L10606. doi:10.1029/2004GL019557.

Chung, C.Y., 1985. Radon variations at Arrowhead and Murietta Springs: continuous and discrete measurements. Pure Appl. Geophys. 122, 294–308.

Chuo, Y.J., Liu, J.Y., Pulinets, S.A., Chen, Y.I., 2002. The ionospheric perturbations prior to the Chi–Chi and Chia–Yi earthquakes. J. Geodyn. 33, 509–517.

Claesson, L., Skelton, A., Graham, C., Dietl, C., Mörth, M., Torssander, P., Kockum, I., 2004. Hydrogeochemical changes before and after a major earthquake. Geology 32, 641–644.

Clark, B., 1981. Stress anomaly accompanying the 1979 Lytle Creek earthquake: implications for earthquake prediction. Science 211, 51–53.

Craig, H., 1980. Fluid-phase earthquake precursor studies n southern California. Trans.-Am. Geophys. Union 61, 1035.

Dal Moro, G., Zadro, M., 1999. Remarkable tilt-strain anomalies preceding two seismic events in Friuli (NE Italy): their interpretation as precursors. Earth Planet. Sci. Lett. 170, 119–129.

Davies, K., Baker, D.M., 1965. Ionospheric effects observed around the time of the Alaskan earthquake of March 28, 1964. J. Geophys. Res. 70, 2251–2253.

Dea, J.Y., Hansen, P.M., Boerner, W.M., 1993. Long-term ELF background noise measurements, the existence of window regions, and applications to earthquake precursor emission studies. Phys. Earth Planet. Inter. 77, 109–125.

Dieterich, J.H., 1972. Time-dependent friction in rocks. J. Geophys. Res. 77, 3690–3697.

Dieterich, J.H., 1978. Time-dependent friction and the mechanics of stick slip. Pure Appl. Geophys. 116, 790–806.

Dieterich, J.H., 1979. Modeling of rock friction, 1. Experimental results and constitutive equations. J. Geophys. Res. 84, 2161–2168.

Draganov, A.B., Inan, U.S., Taranenko, Yu.N., 1991. ULF magnetic signatures at the Earth's surface due to ground water flow: a possible precursor to earthquakes. Geophys. Res. Lett. 18, 1127–1130.

Dragoni, M., Bonafede, M., Boschi, E., 1985. On the interpretation of slow ground deformation precursory to the 1976 Friuli earthquake. Pure Appl. Geophys. 122, 781–792.

Eftaxias, K., Kapiris, P., Dologlou, E., Kopanas, J., Bogris, N., Antonopoulos, G., Peratzakis, A., Hadjicontis, V., 2001a. EM anomalies before the Kozani earthquake: a study of their behavior through laboratory experiments. Geophys. Res. Lett. 29 (8).

Eftaxias, K., Kapiris, P., Polygiannakis, J., Bogris, N., Kopanas, J., Antonopoulos, G., Peratzakis, A., Hadjicontis, V., 2001b. Signature of pending earthquake from electromagnetic anomalies. Geophys. Res. Lett. 29, 3321–3324.

Eftaxias, K., Kapiris, P., Dologlou, E., Kopanas, J., Bogris, N., Antonopoulos, G., Peratzakis, A., Hadjicontis, V., 2002. EM anomalies before the Kozani earthquake: a study of their behavior through laboratory experiments. Geophys. Res. Lett. 29 (8), 1228. doi:10.1029/2001GL013786.

Enescu, B.D., Enescu, D., Constantin, A.P., 1999. The use of electromagnetic data for short-term prediction of Vrancea (Romania) earthquakes: preliminary data. Earth Planets and Space 51, 1099–1117.

Enomoto, Y., Tsutsumi, A., Fujinawa, Y., Kasahara, M., Hashimoto, H., 1997. Candidate precursors: pulse-like geoelectric signals possibly related to recent seismic activity in Japan. Geophys. J. Int. 131, 485–494.

Enomoto, Y., Fujinawa, Y., Hata, M., Hayakawa, M., Kushida, Y., Maeda, K., Nagao, T., Oike, K., Okamoto, T., Uyeda, S., 1998. Possible electromagnetic precursors for 1995 Hyogo-ken Nanbu (Kobe) earthquake. Eos, Trans. Am. Geophys. Union 79, 590.

Fedotov, S.A., Maguskin, M.A., Kirienko, A.P., Zharinov, N.A., 1992. Vertical ground movements on the coast of the Kamchatka Gulf: their specific features in the epicentral zone of the August 17, 1983,earthquake $M = 6.9$, before and after. Tectonophysics 202, 163–167.

Fenoglio, M.A., Johnston, M.J.S., Byerlee, J., 1994a. Magnetic and electric fields associated with changes in high pore pressure in fault zones: application to the Loma Prieta ULF emissions. J. Geophys. Res. 100, 12951–12958.

Fenoglio, M.A., Johnston, M.J.S., Byerlee, J., 1994b. Magnetic and electric fields associated with changes in high pore pressure in fault zones: application to the Loma Prieta ULF emissions. U.S. Geol. Surv. Open File Rep. 94–228, 262–278.

Fitterman, D.V., 1978. Electrokinetic and magnetic anomalies associated with dilatant regions in a layered Earth. J. Geophys. Res. 83, 5923–5928.

Fenoglio, M.A., Johnston, M.J.S., Byerlee, J.D., 1995. Magnetic and electric fields associated with changes in high pore pressure in fault zones: application to the Loma Prieta ULF emissions. J. Geophys. Res. 100, 12951–12958.

Fitterman, D.V., 1979. Theory of electrokinetic–magnetic anomalies in a faulted half-space. J. Geophys. Res. 84, 6031–6040.

Fleischer, R.L., 1981. Dislocation model for radon response to distant earthquakes. Geophys. Res. Lett. 8, 477–480.

Fleischer, R.L., Mogro-Campero, A., 1985. Association of subsurface radon changes in Alaska and the northeastern United States with earthquakes. Geochim. Cosmochim. Acta 49, 1061–1071.

Flores Humanante, B., Giroletti, E., Idrova, J., Monnin, M., Pasinetti, R., Seidel, J.L., 1990. Radon signals related to seismic activity in Ecuador, March 1987. Pure Appl. Geophys. 132, 505–520.

Fraser-Smith, A.C., Bernardi, A., McGill, P.R., Ladd, M.E., Helliwell, R.A., Villard Jr., O.G., 1990. Low-frequency magnetic field measurements near the epicenter of the Ms 7.1 Loma Prieta earthquake. Geophys. Res. Lett. 17, 1465–1468.

Fujii, Y., Nakane, K., 1997. Reevaluation of anomalous crustal movement associated with the 1964 Niigata, Japan, earthquake. Pure Appl. Geophys. 149, 115–127.

Fujinawa, Y.M., Takahashi, K., 1990. Emission of electromagnetic radiation preceding the Ito seismic swarm of 1989. Nature 347, 376–378.

Fujinawa, Y.M., Takahashi, K., 1998. Electromagnetic radiations associated with major earthquakes. Phys. Earth Planet. Inter. 105, 249–259.

Fujiwara, H., Kamogawa, M., Ikeda, M., Liu, J.Y., Sakata, H., Chen, Y.I., Ofuruton, H., Muramatsu, S., Chuo, Y.J., Ohtsuki, Y.H., 2004. Atmospheric anomalies observed during earthquake occurrence. Geophys. Res. Lett. 31, L17110.

Gershenzon, N., Gokhberg, M., 1993. On the origin of electrotelluric disturbances prior to an earthquake in kalamata, Greece. Tectonophysics 224, 169–174.

Gogatishvili, Ya.M., 1984. Geomagnetic precursors of strong earthquakes in the spectrum of geomagnetic pulsations with frequencies of 1–0.02 Hz. Geomagn. Aeronomy 24, 574–576.

Gokhberg, M.B., Morgounov, V.A., Yoshino, T., Tomizawa, I., 1982. Experimental measurements of electromagnetic emissions possibly related to earthquakes in Japan. J. Geophys. Res. 87, 7824–7828.

Golenetskii, S.I., Dem'yanovitch, M.G., Semenov, R.M., Vas'ko, V.G., Avdeev, V.A., Kashkin, V.F., Misharina, L.A., Serebrennikov, S.P., 1982. Seismicity of the regions of the Orongoi basins and the earthquake of 2 October 1980 in western Transbaikal. Sov. Geol. Geophys. 23, 39–46.

Hamilton, R.M., 1975. Earthquake studies in China — a massive earthquake prediction effort is under way. Earthquake Inf. Bull. 7, 3–8.

Hauksson, E., Goddard, J.G., 1981. Radon earthquake precursor studies in Iceland. J. Geophys. Res. 86, 7037–7054.

Hauksson, E., 1981. Radon content of groundwater as an earthquake precursor: evaluation of worldwide data and physical basis. J. Geophys. Res. 86, 9397–9410.

Hayakawa, M., Kawate, R., Molchanov, O.A., Yumoto, K., 1996. Results of ultra-low-frequency magnetic field measurements during the Guam earthquake of 8 August 1993. Geophys. Res. Lett. 23, 241–244.

Hayakawa, M., Ito, T., Smirnova, N., 1999. Fractal analysis of ULF geomagnetic data associated with the Guam earthquake of August 8, 1993. Geophys. Res. Lett. 26, 2797–2800.

Holub, R.F., Brady, B.T., 1981. The effect of stress on radon emanation from rock. J. Geophys. Res. 86, 1776–1784.
Igarashi, G., Wakita, H., 1990. Groundwater radon anomalies associated with earthquakes. Tectonophysics 180, 237–254.
Igarashi, G., Wakita, H., Notsu, K., 1990. Groundwater observations at KSM site in northeast Japan: a most sensitive site to earthquake occurrence. Tohoku Geophys. J. 33, 163–175.
Igarashi, G., Wakita, H., Sato, T., 1992. Precursory and coseismic anomalies in well water levels observed for the February 2, 1992 Tokyo Bay earthquake. Geophys. Res. Lett. 19, 1583–1586.
Igarashi, G., Saeki, S., Takahata, N., Sumikawa, K., Tasaka, S., Sasaki, Y., Takashasi, M., Sano, Y., 1995. Ground-water radon anomaly before the Kobe earthquake in Japan. Science 269, 60–61.
Igarashi, G., Wakita, H., Umeda, K., 1996. Precursory and coseismic changes in well water levels observed for some large earthquakes in Japan. Eos, Trans.-Am. Geophys. Union 77, 457.
Ihmle, P.F., Jordan, T.H., 1994. Teleseismic search for slow precursors to large earthquakes. Science 266, 1547–1551.
Ishankulov, R.I., Kalugin, G.P., 1976. On water level changes within the Bukantaus mountain massif during the Gazli earthquake. In: Mavlyanov, G.A. (Ed.), Earthquake Hazard Zoning and Search for Earthquake Precursors. FAN, Tashkent, pp. 65–66 (in Russian).
Iwatsubo, E.Y., Mortensen, C.E., 1979. Short-term tilt anomalies preceding three local earthquakes near San Jose, California. Eos, Trans.-Am. Geophys. Union 60, 319.
Jiang, F.L., Li, G.R., 1981. The application of geochemical methods in earthquake prediction in China. Geophys. Res. Lett. 8, 469–472.
Jiang, F.L., Li, G.R., Kellogg, W.K., 1981. Experimental studies of the mechanisms of seismo-geochemical precursors. Geophys. Res. Lett. 8, 473–476.
Johnston, M.J.S., Mortensen, C.E., 1974. Tilt precursors before earthquakes on the San Andreas Fault, California. Science 186, 1031–1034.
Jones, L., Molnar, P., 1976. Frequency of foreshocks. Nature 262, 677–679.
Jones, A.C., Johnston, M.J.S., Daul, W., Mortensen, C.E., 1977. Tilt near an earthquake (ML = 4.3), Briones Hills, California. Eos, Trans.-Am. Geophys. Union 58, 1227.
Karakelian, D., Klemperer, S.L., Fraser-Smith, A.C., Thompson, G.A., 2002. Ultra-low frequency electromagnetic measurements associated with the 1988 MW 5.1 San Juan Bautista, California earthquake and implications for mechanisms of electromagnetic earthquake precursors. Tectonophysics 359, 65–79.
Kawabe, I., 1984. Anomalous changes of CH_4/Ar ratio in subsurface gas bubbles as seismogeochemical precursors at Matsuyama. Japan, Pure Appl. Geophys. 122, 194–214.
Kawabe, I., Ohno, I., Nadano, S., 1988. Groundwater flow records indicating earthquake occurrence and induced Earth's free oscillations. Geophys. Res. Lett. 15, 1235–1238.
King, C.Y., 1978. Radon emanation on San Andreas Fault. Nature 271, 516–519.
King, C.Y., 1980. Episodic radon changes in subsurface soil gas along active faults and possible relation to earthquakes. J. Geophys. Res. 85, 3065–3078.
King, C.Y., 1985. Radon monitoring for earthquake prediction in China. Earthqu. Predict. Res. 3, 47–68.
King, C.Y., Azuma, S., Ohno, M., Asai, Y., He, P., Kitagawa, Y., Igarashi, G., Wakita, H., 2000. In search of earthquake precursors in the water-level data of 16 closely clustered wells at Tono. Japan, Geophys. J. Int. 143, 469–477.
Kissin, I.G., Barabanov, V.L., Grinevsky, A.O., Markov, V.M., Khudzinsky, L.L., 1984a. Experimental investigations into conditions of ground water in order to intensify hydrodynamic earthquake forerunners. Izv. Acad. Sci. USSR, Phys. Earth 6, 74–86 (in Russian).
Kissin, I.G., Barabanov, V.L., Grinevsky, A.O., Khudzinsky, L.L., 1984b. Variation of groundwater level in the western Fergana Valley. In: Nikolaev, A.V., Kissin, I.G. (Eds.), Hydrogeodynamic Earthquake Precursors. InNauka, Moscow, pp. 96–119 (in Russian).
Kissin, I.G., Grinevsky, A.O., 1990. Main features of hydrogeodynamic earthquake precursors. Tectonophysics 178, 277–286.
Koizumi, N., Tsukuda, E., Kamigaichi, O., Matsumoto, N., Takahashi, M., Sato, T., 1999. Preseismic changes in groundwater level and volumetric strain associated with earthquake swarms of the east coast of Izu Peninsula. Japan Geophys. Res. Lett. 31, L10606. doi:10.1029/2004GL019557.
Koizumi, N., Kitagawa, Y., Matsumoto, N., Takahashi, M., Sato, T., Kamigaichi, O., Nakamura, K., 2004. Preseismic groundwater level changes induced by crustal deformations related to earthquake swarms of the east coast of the Izu Peninsula. Japan, Geophys. Res. Lett. 26, 3509–3512.
Kopytenko, Y.A., Matiashvili, T.G., Voronov, P.M., Kopytenko, E.A., Molchanov, O.A., 1993. Detection of ultra-low-frequency emissions connected with the Spitak earthquake and Its aftershock activity, based on geomagnetic pulsations data at Dusheti and Vardzia observatories. Phys. Earth Planet. Inter. 77, 85–95.
Kovach, R.L., Nur, A., Wesson, R.L., Robinson, R., 1975. Water-level fluctuation and earthquakes on the San-Andreas Fault Zone. Geology 3, 437–456.
Lachenbruch, A.H., Sass, J.H., 1992. Heat flow from Cajon Pass, fault strength and tectonic implications. J. Geophys. Res. 97, 4995–5015.
Langbein, J., Borcherdt, R., Dreger, D., Fletcher, J., Hardebeck, J.L., Hellweg, M., Ji, C., Johnston, M., Murray, J.R., Nadeau, R., Rymer, M.J., Treiman, J.A., 2005. Preliminary report on the 28 September 2004 M 6.0 Parkfield, California earthquake. Seismol. Res. Lett. 76, 10–26.
Larkina, V.I., Nalivayko, A.V., Gershenzon, N.I., Gokhberg, M., Liperovskiy, V.A., Shalimov, S.L., 1984. Observation of VLF emission, related with seismic activity, on the Interkosmos-19 satellite. Geomagn. Aeronomy 23, 684–687.
Larkina, V.I., Migulin, V.V., Molchanov, O.A., Kharkov, I.P., Inchin, A.S., Schvetcova, V.B., 1989. Some statistical results on very low frequency radiowave emissions in the upper ionosphere over earthquake zones. Phys. Earth Planet. Inter. 57, 100–109.
Leary, P.C., Malin, P.E., 1984. Ground deformation events preceding the Homestead Valley earthquakes. B. Seismol. Soc. Am. 74, 1799–1817.
Liang, W., 1980. Anomalous fluorine variations in groundwater as earthquake precursors. Eos, Trans.-Am. Geophys. Union 61, 1035.
Linde, A., Suyehiro, K., 1983. Strain changes preceding two large earthquakes near the Izu Peninsula, Japan. Eos, Trans.-Am. Geophys. Union 64, 313.
Linde, A.T., Suyehiro, K., Miura, S., Selwyn Sacks, I., Takagi, A., 1988. Episodic aseismic earthquake precursors. Nature 334, 513–515.
Lisowski, M., Prescott, W.H., Savage, J.C., Svarc, J.L., 1990. A possible geodetic anomaly observed prior to the Loma Prieta, California earthquake. Geophys. Res. Lett. 17, 1211–1214.
Liu, J.Y., Chen, Y.J., Pulinets, S.A., Tsai, Y.B., Chuo, Y.J., 2000. Seismo-ionospheric signatures prior to M?6.0 Taiwan earthquakes. Geophys. Res. Lett. 27, 3113–3116.
Liu, K.K., Tsai, Y.B., Yeh, Y.H., Yui, T.F., Teng, T.L., 1983. Anomalous groundwater radon changes and possible correlation with earthquakes in northern Taiwan. Eos, Trans.-Am. Geophys. Union 64, 758.
Liu, K.K., Yui, T.F., Yeh, Y.H., Tsai, Y.B., Teng, T.L., 1985. Variations of radon content in ground waters and possible correlation with seismic activities in northern Taiwan. Pure Appl. Geophys. 122, 231–244.
Lomnitz, C., 1994. Fundamentals of Earthquake Prediction. John Wiley & Sons, New York. (326 pp.).
Lorenzetti, E., Tullis, T.E., 1989. Geodetic predictions of a strike-slip fault model: Implications for intermediate- and short-term earthquake prediction. J. Geophys. Res. 94, 12,343–12,361.
Maeda, K., Tokimasa, N., 1996. Decametric radiation at the time of the Hyogo-ken Nanbu earthquake near Kobe in 1995. Geophys. Res. Lett. 23, 2433–2436.
Martinelli, G., 2000. Contributions to a history of earthquake prediction research. Seism. Res. Lett. 71, 583–603.
Mavlyanov, S.R., Sultankhodzhaev, A.N., 1981. Anomalous variations of groundwater hydrogeochemical parameters in eastern Fergana: precursor to the February 2, 1978 Alai earthquake. Uzb. Geol. Z. 2, 9–13 (in Russian).
Mazzella, A., Morrison, H.F., 1974. Electrical resistivity variations associated with earthquakes on the San Andreas Fault. Science 185, 855–857.
Merifield, P.M., Lamar, D.L., 1981. Anomalous water-level changes and possible relation with earthquakes. Geophys. Res. Lett. 8, 437–440.
Mil'kis, M.R., 1984. Hydrogeological precursors of the 1948 Ashkhabad earthquake. In: Nikolaev, A.V., Kissin, I.G. (Eds.), Hydrogeodynamic Earthquake Precursors. Nauka, Moscow, pp. 76–95 (in Russian).
Mil'kis, M.R., Voronin, I.V., 1983. Methodological principles in the planning of hydrogeological studies for prediction of large earthquakes. In: Vartanyan, G.S. (Ed.), Summaries of Reports at the All-Union Sciences and Technology Seminar, March 24–25, 1983, "Methodology and Observations of Groundwater Behaviour for Earthquake Prediction". VSEGINGEO, Moscow, pp. 15–17 (in Russian).
Mogi, K., 1985. Temporal variation of crustal deformation during the days preceding a thrust-type great earthquake — the 1944 Tonankai earthquake of magnitude 8.1. Japan, Pure Appl. Geophys. 122, 765–780.
Mogi, K., Mochizuki, H., Kurokawa, Y., 1989. Temperature changes in an artesian spring at Usami in the Izu Peninsula (Japan) and their relation to earthquakes. Tectonophysics 159, 95–108.
Molchanov, O.A., Kopytenko, Y.A., Voronov, P.M., Kopytenko, E.A., Matiashvili, T.G., Fraser-Smith, A.C., Bernardi, A., 1992. Results of ULF magnetic field measurements near the epicenters of the Spitak (Ms = 6.9) and Loma Prieta (Ms = 7.1) earthquakes: comparative analysis. Geophys. Res. Lett. 19, 1495–1498.
Molchanov, O.A., Hayakawa, M., Ondoh, T., Kanai, E., 1998. Precursory effects in the subionosphere VLF signals for the Kobe earthquake. Phys. Earth Planet. Inter. 105, 239–248.
Monakhov, F.I., 1981. Comparative characterization of earthquake preparation at different depths. Dokl. Akad. Nauk SSSR 261, 458–460 (in Russian).
Monakhov, F.I., Khantaev, A.M., Saprygin, S.M., 1979. A Short-Term Precursor and Its Relation to Elastic Crustal Strain. Yuzhno-Sakhalinsk. (16 pp. in Russian).
Monakhov, F.I., Kissin, I.G., Khantaev, A.M., Saprygin, S.M., Grishechkin, B.A., 1980. New evidence of the hydrogeodynamic effect preceding earthquakes. Izv. Acad. Sci. U.S.S. R., Phys. Earth 1, 105–107 (in Russian).
Mortensen, C.E., Johnston, M.J.S., 1976. Anomalous tilt preceding the Hollister earthquake of November 28, 1974. J. Geophys. Res. 81, 3561–3566.
Mueller, R.J., Johnston, M.J.S., 1990. Seismomagnetic effect generated by the October 18, 1989, ML 7.1 Loma Prieta, California, earthquake. Geophys. Res. Lett. 23, 241–244.
Nagamine, K., Sugisaki, R., 1991a. Coseismic changes of subsurface gas compositions disclosed by an improved seismo-geochemical system. Geophys. Res. Lett. 18, 2221–2224.
Neresov, I.L., Latynina, L.A., 1992. Strain processes before the Spitak earthquake. Tectonophysics 202, 221–225.
Nourbehecht, B. (1963). Irreversible thermodynamic effects in inhomogeneous media and their applications in certain geoelectric problems, Ph.D. thesis, Mass. Inst. of Technol., Cambridge.
O'Neil, J.R., King, C.Y., 1980. Deuterium anomalies in groundwater as precursors to seismic activity in California. Eos, Trans.-Am. Geophys. Union 61, 1033.
Ogawa, T., Oike, K., Miura, T., 1985. Electromagnetic radiation from rocks. J. Geophys. Res. 90, 6245–6249.
Ohno, M., Wakita, H., 1996. Coseismic radon changes of the 1995 Hyogo-ken Nanbu earthquake. J. Phys. Earth 44, 391–395.
Ondoh, T., 1998. Ionospheric disturbances associated with great earthquake of Hakkaido southwest coast, Japan of July 12, 1993. Phys. Earth Planet. Inter. 105, 261–269.
Orolbaev, E.E., 1984. First results in the study of groundwater behaviour in a search for hydrogeodynamic earthquake precursors. In: Nikolaev, A.V., Kissin, I.G. (Eds.), Hydrogeodynamic Earthquake Precursors. Nauka, Moscow, pp. 50–65 (in Russian).

Ospanov, A.B., Mizev, V.A., 1985. Hyrdrogeochemical Features of the Alma-Ata Seismic Zone. Nauka Kazakhskoi SSR, Alma-Ata. (128 pp. in Russian).
Parrot, M., 1994. Statistical study of ELF/VLF emissions recorded by a low-altitude satellite during seismic events. J. Geophys. Res. 99, 23,339–23,347.
Perez, N.M., 1996. Precursory hydrogeochemical signatures of the 1996 Perpignan earthquake, France. Eos, Trans.-Am. Geophys. Union 77, 457.
Pierce, E.T., 1976. Atmospheric electricity and earthquake prediction. Geophys. Res. Lett. 3, 185–188.
Press, F., Siever, R., 1978. Earth, 2nd Edition. W.H. Freeman, San Francisco. (649 pp.).
Qiang, Z.J., Xu, X.D., Dian, C.G., 1997. Thermal infrared anomaly precursor of impending earthquakes. Pure Appl. Geophys. 149, 159–171.
Raleigh, C.B., Molnar, P., Hanks, T., Nur, A., Wu, F., Savage, J., Scholz, C., Craig, H., Turner, R., Bennett, G., 1977. Prediction of the Haicheng earthquake. Eos, Trans. Am. Geophys. Union 58, 236–272.
Reasenberg, P.A., 1999. Foreshock occurrence before large earthquakes. J. Geophys. Res. 104, 4755–4768.
Reddy, D.V., Sukhija, B.S., Nagabhushanam, P., Kumar, D., 2004. A clear case of radon anomaly associated with a microearthquake event in a stable continental region. Geophys. Res. Lett. 31, L10609. doi:10.1029/2004GL019971.
Redondo, R., Trujillo, I., Hernandez, P.A., Salazar, J.M., Perez, N.M., Nakai, S., Wakita, H., 1996. Hydrochemical and isotopic secular variations and relation to the 1995 Galicia earthquakes, Spain. Eos, Trans.-Am. Geophys. Union 77, 457.
Reimer, G.M., 1980. Variations in soil–gas helium concentrations corresponding to recent central California earthquakes. Eos, Trans.-Am. Geophys. Union 61, 1034.
Reimer, G.M., 1990. Soil–gas helium increase preceding the Loma Prieta earthquake. Eos, Trans.-Am. Geophys. Union 71, 289.
Rice, J.R., Cleary, M.P., 1976. Some basic stress diffusion solutions for fluid-saturated elastic porous media with compressible constituents. Rev. Geophys. Space Phys. 14, 227–241.
Richon, P., Sabroux, J.C., Halbwachs, M., Vandemeulebrouck, J., Poussielgue, N., Tabbagh, J., Punongbayan, R., 2003. Radon anomaly in the soil of Taal volcano, the Philippines: a likely precursor of the M7.1 Mindoro earthquake (1994). Geophys. Res. Lett. 30, 1481. doi:10.1029/2003GL016902.
Rikitake, T., 1976. Earthquake Prediction. Elsevier, New York. (357 pp.).
Roeloffs, E.A., 1988. Hydrologic precursors to earthquakes: a review. Pure Appl. Geophys. 126, 177–209.
Roeloffs, E.A., Quilty, E., 1997. Water level and strain changes preceding and following the August4, 1985 Kettleman Hills, California, earthquake. Pure Appl. Geophys. 149, 21–60.
Ruina, A.L., 1983. Slip instability and state variable friction laws. J. Geophys. Res. 88, 10,359–10,370.
Sasai, Y., 1991. Tectonomagnetic modeling on the basis of the linear piezomagnetic effect. Bull. Earthq. Res. Inst. Univ. Tokyo 66, 585–722.
Satake, H., Ohashi, M., Hayashi, Y., 1985. Discharge of H2 from the Atotsugawa and Ushikubi faults, Japan, and its relation to earthquakes. Pure Appl. Geophys. 122, 185–193.
Sato, M., Sutton, A.J., McGee, K.A., Russell-Robinson, S.L., 1986. Monitoring of hydrogen along the San Andreas and Calaveras faults in central California in 1980–1984. J. Geophys. Res. 91, 12,315–12,326.
Savage, J.C., 1977. Observations of tilt and self potential a an epicentral distance of 20 km preceding the Haicheng earthquake, (M = 7.3), People's Republic of China. Eos, Trans. Am. Geophys. Union 58, 311.
Scholz, C.H., 1990. The Mechanics of Earthquakes and Faulting. Cambridge U. Press, Cambridge, UK. (439 pp.).
Segovia, N., de la Cruz-Reyna, S., Mena, M., Ramos, E., Monnin, M., Seidel, J.L., 1989. Radon in soil anomaly observed at Los Azufres geothermal field, Michoacan: a possible precursor of the 1985 Mexico earthquake (Ms = 8.1). Nat. Hazards 1, 319–329.
Serebryakova, O.N., Bilichenko, S.V., Chmyrev, V.M., Parrot, M., Rauch, J.L., Lefeuvre, F., Pokhotelov, O.A., 1992. Electromagnetic ELF radiation from earthquake regions as observed from low-altitude satellites. Geophys. Res. Lett. 19, 91–94.
Shalimov, S., Gokhberg, M., 1998. Lithosphere–ionosphere coupling mechanism and its application to the earthquake in Iran on June 20, 1990: a review of ionospheric measurements and basic assumptions. Phys. Earth Planet. Inter. 105, 211–218.
Shapiro, M.H., Melvin, J.D., Tombrello, T.A., Whitcomb, J.H., 1980. Automated radon monitoring at a hard-rock site in the southern California Transverse Ranges. J. Geophys. Res. 85, 3058–3064.
Shapiro, M.H., Rice, A., Mendenhall, M.H., Melvin, J.D., Tombrello, T.A., 1985. Recognition of environmentally caused variations in radon time series. Pure Appl. Geophys. 122, 309–326.
Shi, H., Cai, Z., 1986. Geochemical characteristics of underground fluids in some active fault zones in China. J. Geophys. Res. 91, 12,282–12,290.
Shifflett, H., Witbaard, R., 1996. Multiple precursors to the Landers earthquake. B. Seismol. Soc. Am. 86, 113–121.
Silver, P., 1998. Why is earthquake prediction so difficult? Seism. Res. Lett. 69, 111–113.
Silver, P.G., Valette-Silver, N.J., 1992. Detection of hydrothermal precursors to large northern California earthquakes. Science 257, 1363–1368.
Silver, P.G., Valette-Silver, J.N., Linde, A.T., Kolbek, O., 1990. Detection of a hydrothermal precursor of the Loma Prieta earthquake of Oct. 18, 1989. Eos, Trans.-Am. Geophys. Union 71, 1461.
Smith, B.E., Johnston, M.J.S., 1976. A tectonomagnetic effect observed before a magnitude 5.2 earthquake near Hollister, CA. J. Geophys. Res. 81, 3556–3560.
Soter, Steven, 1999. Macroscopic seismic anomalies and submarine pockmarks in the Corinth–Patras Rift, Greece. Tectonophysics 308, 275–290.
Steele, S.R., 1981. Radon and hydrologic anomalies on the Rough Creek Fault: possible precursors to the M5.1 eastern Kentucky Earthquake, 1980. Geophys. Res. Lett. 8, 465–468.
Steele, S.R., 1984. Anomalous radon emanation at local and regional distances preceding earthquakes in the New Madrid Seismic Zone and adjacent areas of the central Mid-Continent of North America 1981–1984. Pure Appl. Geophys. 122, 353–368.
Sugisaki, R., 1978. Changing He/Ar and N2/Ar ratios of fault air may be earthquake precursors. Nature 275, 209–211.
Sugisaki, R., Sugiura, T., 1985. Geochemical indicator of tectonic stress resulting in an earthquake in central Japan, 1984. Science 229, 1261–1262.
Sugisaki, R., Sugiura, T., 1986. Gas anomalies at three mineral springs and a fumarole before an inland earthquake, central Japan. J. Geophys. Res. 91, 12,296–12,304.
Sugisaki, R., Ito, T., Nagamine, K., Kawabe, I., 1996. Gas geochemical changes at mineral springs associated with the 1995 southern Hyogo earthquake (M = 7.2), Japan, Earth Planet. Sci. Lett. 139, 239–249.
Sultankhodzhaev, A.N., Chernov, I.G., 1978. Seismological earthquake precursors: variations of groundwater hydrogeodynamic parameters. Uzb. Geol. Z. 4, 3–7 (in Russian).
Sultankhodzhaev, A.N., Azizov, G.Y.u., Latypov, S.V., Zigan, F.G., Arifbaev, A.K.h., 1986. Hydroseismological precursors of the Dzhirgatal earthquake based on studies conducted in the Fergana Prediction Test Area. Uzb. Geol. Z. 3, 7–12 (in Russian).
Teng, T.L., 1980. Some recent studies on groundwater radon content as an earthquake precursor. J. Geophys. Res. 85, 3089–3099.
Teng, T.L., Sun, L.F., 1986. Research on groundwater radon as a fluid phase precursor to earthquakes. J. Geophys. Res. 91, 12,305–12,313.
Thomas, D., 1988. Geochemical precursors to seismic activity. Pure Appl. Geophys. 126, 241–266.
Toutain, J.P., Baubron, J., 1999. Gas geochemistry and seismotectonics: a review. Tectonophysics 304, 1–27.
Toutain, J.P., Munoz, M., Poitrasson, F., Lienard, A.C., 1997. Springwater chloride ion anomaly prior to a ML = 5.2 Pyrenean earthquake. Earth Planet. Sci. Lett. 149, 113–119.
Tse, S.T., Rice, J.R., 1986. Crustal earthquake instability in relation to the depth variation of frictional slip properties. J. Geophys. Res. 91, 9452–9472.
Tsunogai, U., Wakita, H., 1995. Precursory chemical changes in groundwater: Kobe earthquake, Japan. Science 269, 61–63.
Tsunogai, U., Wakita, H., 1996. Anomalous changes in groundwater chemistry: possible precursors of the 1995 Hyogo-ken Nanbu earthquake. Japan. J. Phys. Earth 44, 381–390.
Ui, H., Moriuchi, H., Takemura, Y., Tsuchida, H., Fujii, I., Nakamura, M., 1988. Anomously high radon discharge from the Atotsugawa Fault prior to the western Nagano prefecture earthquake (M6.8) of September 14, 1984. Tectonophysics 152, 147–152.
Valette-Silver, N.J., Silver, P.G., 1991. Detection of hydrothermal precursors to northern California earthquakes. Eos, Trans.-Am. Geophys. Union 72, 202.
Varotsos, P., Alexopoulos, K., 1984. Physical properties of the variations of the electric field of the Earth preceding earthquakes, I. Tectonophysics 110, 73–98.
Varshal, G.M., Sobolev, G.A., Barsukov, V.L., Koltsov, A.V., Kostin, B.I., Kudinova, T.F., Stakheyev, Y.I., Tretyakova, S.P., 1985. Separation of volatile components from rocks under mechanical loading as the source of hydrogeochemical anomalies preceding earthquakes. Pure Appl. Geophys. 122, 463–477.
Virk, H.S., Singh, B., 1993. Radon anomalies in soil–gas and groundwater as earthquake precursor phenomena. Tectonophysics 227, 215–224.
Virk, H.S., Baljinder, S., 1994. Radon recording of Uttarkashi earthquake. Geophys. Res. Lett. 21, 737–740.
Virk, H.S., Baljinder, S., 1995. Correlation of radon anomalies with the Uttarkashi earthquake. Geol. Soc. India Bull. 30, 125–132.
Virk, H.S., Walia, V., Kumar, N., 2001. Helium/radon precursory anomalies of Chamoli earthquake, Garhwal Himalaya, India. J. Geodyn. 31, 201–210.
Wakita, H., 1984. Groundwater observations for earthquake prediction in Japan. A Collection of Papers of International Symposium on Continental Seismicity and Earthquake Prediction (ISCSEP) (Seismological Press, Beijing), pp. 494–500.
Wakita, H., Nakamura, Y., Notsu, K., Noguchi, M., Asada, T., 1980. Radon anomaly: a possible precursor to the 1978 Izu–Oshima–kinkai earthquake. Science 207, 882–883.
Wakita, H., Nakamura, Y., Sano, Y., 1988. Short-term and intermediate-term geochemical precursors. Pure Appl. Geophys. 126, 267–278.
Wakita, H., Igarashi, G., Nakamura, Y., Sano, Y., Notsu, K., 1989. Coseismic radon changes in groundwater. Geophys. Res. Lett. 16, 417–420.
Wakita, H., Igarashi, G., Notsu, K., 1991. An anomalous radon decrease in groundwater prior to an M6.0 earthquake: a possible precursor? Geophys. Res. Lett. 18, 629–632.
Wallace, R.E., Teng, T.L., 1980. Prediction of the Sungpan–Pingwu earthquakes, August 1976, B. Seismoc. Soc. Am. 70, 1199–1223.
Wang, C., Wang, Y., Guo, Y., 1984a. Some results of groundwater level observation in earthquake areas in China during the past 15 years. In: Gu Congxu, Ma Xingyuan (Eds.), A Collection of Papers of the International Symposium on Continental Seismicity and Earthquake Prediction. Seismological Press, Beijing, China, pp. 501–513.
Wang, C., Wang, Y., Zhang, H., Li, Y., Zhao, S., 1984b. Characteristics of water level variation in deep wells before and after the Tangshan earthquake. In: Evison, F.F. (Ed.), Proceedings of an Internal Symposium on Earthquake Prediction, Terra. Tokyo/Unesco, Paris, pp. 215–232.
Warwick, J.W., Stoker, C., Meyer, T.R., 1982. Radio emission associated with rock fracture: possible application to the great Chilean earthquake of May 22, 1960. J. Geophys. Res. 87, 2851–2859.
Working Group on California Earthquake Probabilities (1988). Probabilities of Large Earthquakes Occurring in California on the San Andreas Fault, United States Geological Survey Open-File Report 88-398, Reston, VA, 62 pp.
Wyss, M., Klein, F.W., Johnston, A.C., 1981. Precursors to the Kalapana M7.2 earthquake. J. Geophys. Res. 86, 3881–3900.

Yamaguchi, R., 1980. Changes in water-level on Funabara and Kakigi before the Izu–Kanto–Toho–Ohi earthquake of 1980. Bull. Earthq. Res. Inst. Univ. Tokyo 55, 1065–1071.
Yépez, E., Angulo-Brown, F., Peralta, J.A., Pavía, C.G., González-Santo, G., 1995. Electric field patterns as seismic precursors. Geophys. Res. Lett. 22, 3087–3090.
Yoshino, T., Tomizawa, I., Sugimoto, T., 1993. Results of statistical analysis of low-frequency seismogenic EM emissions as precursors to earthquakes and volcanic eruptions. Phys. Earth Planet. Inter. 77, 21–31.
Yu, G.K., Mitchell, B.J., 1988. A study of the non-tectonic influences on groundwater level fluctuations. Proc. Geol. Soc. China 31, 111–124.
Zhao, Y., Qian, F., 1994. Geoelectric precursors to strong earthquakes in China. Tectonophysics 233, 99–113.
Zhukov, V.S., Lykov, V.I., Sukhomlin, V.F., 1978. Some results of electrometric observations in the Ashkabad Geodynamical Test Area, Izv. Akad. Nauk Turk. SSR, Phys.-Tech. Chem. Geol. Sci. 2, 41–46 (in Russian).